VYSOKÉ UČENÍ TECHNICKÉ V BRNĚ

BRNO UNIVERSITY OF TECHNOLOGY

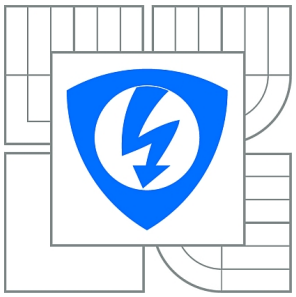

FAKULTA ELEKTROTECHNIKY A KOMUNIKAČNÍCH TECHNOLOGIÍ

ÚSTAV MIKROELEKTRONIKY

FACULTY OF ELECTRICAL ENGINEERING AND COMMUNICATION

DEPARTMENT OF MICROELECTRONICS

DESIGN AND SIMULATION OF MICRO-BOLOMETER IN MEMS TECHNOLOGY

NÁVRH A SIMULACE ČIPU MIKROBOLOMETRU V MEMS TECHNOLOGII

DIPLOMOVÁ PRÁCE

MASTER'S THESIS

AUTOR PRÁCE — Bc. VOJTĚCH SVATOŠ

AUTHOR

VEDOUCÍ PRÁCE — doc. Ing. JAROMÍR HUBÁLEK, Ph.D.

SUPERVISOR

BRNO 2014

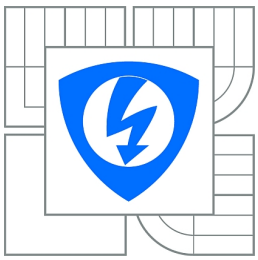

VYSOKÉ UČENÍ TECHNICKÉ V BRNĚ

Fakulta elektrotechniky a komunikačních technologií

Ústav mikroelektroniky

Diplomová práce

magisterský navazující studijní obor
Mikroelektronika

Student:	Bc. Vojtěch Svatoš	***ID:***	119617
Ročník:	2	***Akademický rok:***	2013/2014

NÁZEV TÉMATU:

Návrh a simulace čipu mikrobolometru v MEMS technologii

POKYNY PRO VYPRACOVÁNÍ:

Prostudujte problematiku bolometrů pro snímání IR záření. Proveďte teplotně-mechanické simulace struktury bolometru a navrhněte vhodné materiály pro realizaci dle dostupných MEMS technologií. Sestavte úplný technologický postup výroby čipu. Vytvořte design bolometru pro plánovaný technologický postup výroby. Vytvořte náhradní model bolometru vhodný pro stanovení hodnot elektrické odezvy bolometru. Pomocí dostupných technologií realizujte zkušební vzorky a proveďte charakterizaci vyrobených čipů.

DOPORUČENÁ LITERATURA:

Dle doporučení vedoucího práce.

Termín zadání:	10.2.2014	***Termín odevzdání:***	29.5.2014

Vedoucí práce: doc. Ing. Jaromír Hubálek, Ph.D.
Konzultanti diplomové práce:

prof. Ing. Vladislav Musil, CSc.
Předseda oborové rady

UPOZORNĚNÍ:

Abstract

This master thesis studies the infrared detector called bolometer. The task is to improve the infrared detection by using different type of absorption layer modified by the carbon nanotubes. In theoretical part there are basic terms of thermal engineering and basics definitions of bolometer physics. The bolometer design is presented and described. The thermal mechanical simulations are evaluating the operation behavior. PSpice model of bolometer is created combing the thermal and electrical properties of the bolometer chip. The fabrication process is then presented and detailed described.

Keywords

Infrared detectors, microbolometer, thermal engineering, design, fabrication process, simulation.

Abstrakt

Tato diplomová práce zkoumá problematiku detektoru infračerveného záření nazývaného bolometr. Cílem je pokrok v detekci infračerveného záření použitím odlišné absorpční vrstvy modifikovanou karbonovými nanotrubicemi. V teoretické části jsou uvedeny základní fyzikální pojmy z problematiky teplotního managmentu a základních fyzikálních vztahů bolometru. Design bolometru je představen a popsán. Teplotně mechanické simulace předvídají chování bolometru při detekci infračerveného záření. PSpice model je vytvořen a kombinuje termální a elektrické vlastnosti čipu bolometru. Dále je uveden proces výroby bolometru, které je detailně popsán.

Klíčová slova

Detektory infračerveného záření, mikrobolometr, teplotní managment, design, výrobní proces, simulace.

Citation:

SVATOŠ, V. *Design and Simulation of Micro-Bolometer in MEMS Technology*. Brno: Vysoké učení technické v Brně, Fakulta elektrotechniky a komunikačních technologií, 2014. 57 s. Vedoucí diplomové práce doc. Ing. Jaromír Hubálek, Ph.D.

Author Declaration

I declare that I wrote this master thesis by myself, independently, and I work under the direction of master thesis supervisor, using the cited sources, literature and other information sources which all are listed in the reference part of thesis. As author of this work, I declare I have not violated any owner rights of third person, namely I have not proceed with any way breaking the law during writing this thesis. I am fully aware of consequences resulting from these terms violation.

In Brno 28th May 2014 Signature

Acknowledgment

First of all, I would like to thank my thesis supervisor doc. Ing. Jaromir Hubalek, Ph.D., for his methodical leading, all discussions, and consultation which made this thesis possible. I am especially grateful to my colleagues from LabSensNano and mainly to Pavel Neuzil, for their continuing help and support during this work realization. Finally, I would like to thanks to my family for all their support, help, and motivation.

SIX research centre
sensor, information and communication systems

Faculty of Electrical Engineering
and Communication

Brno University of Technology
Technicka 12, CZ-61600 Brno, Czechia

http://www.six.feec.vutbr.cz

Experimentální část této diplomové práce byla realizována na výzkumné infrastruktuře vybudované v rámci projektu CZ.1.05/2.1.00/03.0072
Centrum senzorických, informačních a komunikačních systémů (SIX)
operačního programu Výzkum a vývoj pro inovace.

MINISTERSTVO ŠKOLSTVÍ, MLÁDEŽE A TĚLOVÝCHOVY

EVROPSKÁ UNIE
EVROPSKÝ FOND PRO REGIONÁLNÍ ROZVOJ
INVESTICE DO VAŠÍ BUDOUCNOSTI

2007–13
OP Výzkum a vývoj pro inovace

Table of Contents

Table of Contents 6

Introduction 9

1 Theory 11

1.1 Bolometer Definition and Infrared Detectors Classification 11

1.2 Brief History of Bolometer and Infrared Detectors 11

1.3 Basic Physics Terminology for Thermal Engineering 13

1.3.1 Heat Transfer 13

1.3.2 Thermal Conduction 13

1.3.3 Thermal Radiation 14

1.3.4 The Heat Transfer Equation 15

1.4 Bolometer Physics 15

1.4.1 Thermal Detectors 15

1.4.2 Thermal Detection of Uncooled Bolometer 16

1.4.3 Bolometer Physical Description 16

1.4.4 The Self Heating Effect of Bolometer 16

1.4.5 Bolometer System Noise 17

1.5 Bolometer Design 17

1.5.1 Bolometer Chip 17

1.5.2 Focal Plane Arrays 18

1.5.3 Bolometer Temperature Sensing Materials 19

1.6 Read-Out Circuit 20

1.6.1 Read-Out Circuit Using a Wheatstone Bridge 20

2 Absorption Layer Characterization 24

2.1 Theory of FT-IR Measurement 24

2.1.1 Principle of ATR Method 24

2.1.2 Principle of Transmission Spectroscopy Method 24

2.2 Deposition of CNTs Layer 25
2.3 FT-IR Measurement Results and Discussion 26
3 Design of Bolometer Chip 28
3.1 Description of Bolometer Design Cells 28
3.1.1 The Van der Pauw resistivity structure 28
3.1.2 Single Bolometer Cell 30
3.1.3 Cell for Measurement of Titanium Layer Material Properties 30
3.1.4 Cell for SiO_2 Thermal Conductance Measurement 30
3.1.5 Cell for Bolometer Thermal Capacitance Measurement 32
3.1.6 Cell for Measurement of Incident IR radiation 33
3.1.7 Series-Parallel Bolometer Combination Cell 33
4 Thermal Mechanical Simulation and Analysis 34
4.1 Material Properties Used in Simulation 34
4.2 Setting of Fabrication Process 35
4.3 Creating 3-D Model and Mesh Settings 36
4.4 Simulations and Results 37
4.4.1 Solver Settings for Thermal Distribution and Displacement Analyze 38
4.4.2 Results of Thermal Distribution and Displacement Analyze 38
4.4.3 Solver Setting for Steady Time Analyses 40
4.4.4 Results for Steady Time Analyses 40
4.4.5 Solver Setting for Transient Response to Step Voltage 43
4.4.6 Results for Transient Response to Step Voltage Simulation 43
4.5 Chapter Conclusion 44
5 PSpice Model of Bolometer Structure 45
5.1 Electro – Thermal Modeling of IR Bolometer 45
5.2 Settings for Voltage Response Simulation 47
5.3 Simulation Results and Conclusion 48

5.4 Chapter Conclusion 50
6 Fabrication of Bolometer Chip 51
6.1 Fabrication Process Plan Overview 51
6.1.1 CNTs Deposition on the Chip 52
6.2 Fabrication Process Conclusion 53
7 Conclusion 54
8 References 56

Introduction

The uncooled bolometers have become a major device and technology for infrared detection. The improvement of these devices and technology is an important task for today's research. This thesis task is to study design, design, performance, and fabrication of the microbolometer chip using carbon nanotubes as the absorption layer. The CNTs has been never used as the absorption layer so this thesis presents the new approach for IR detection technology.

The theoretical part of thesis deals with the heat transfer physics. The bolometer operation principle is then described, namely the important bolometer parameters affecting its function. The major parameters as thermal conductance, thermal capacitance, and thermal time constant are carefully studied. In the following part, there is shown the commonly used design, and there is overview of some materials employed for infrared detection. The carbon nanotubes are not theoretically studied in this thesis. The read-out circuit for bolometer is briefly described, mainly to understand the important signals which can be detected during bolometer operation.

The characterization of absorption layer is then included in this thesis. There are parameters of the CNTs deposition used to create the absorption layer for measurement. The FT-IR technique has been performed to characterize the samples.

The design which is used for bolometer fabrication is shown in following part. There is information of the bolometer structures, and the fundamental cells. The few types of cells are then shown and revealed. The bolometer characterization measurements are studied in the design part, the specific cell is intended for particular characterization measurement of bolometer chip so after completing of these sort of measurements, the thermal bolometer characterization, and the bolometer value of infrared absorption will be known.

The following part is dealing with the thermal mechanical simulations which have been simultaneously done during designing state so the design could be optimized. The materials properties chosen for the simulation is set up considering the actual fabrication process. The new structure design is presented in this chapter solving the problem with displacement of suspended membrane. The critical electrical thermal parameters of bolometer are evaluated by these simulations.

The PSpice model representing the bolometer structure including thermal parameters is then created. The simulation of measurement circuit is performed in the order to design the suitable circuit for to characterize of actual bolometers. The bolometer serial parallel combinations have been investigated in this chapter considering the improving of the bolometer sensitivity for IR detection.

The fabrication process is the final part of this thesis. The fabrication process plan is described explaining the particular technologies for each layer of structure which is to be fabricated. The new technology process for deposition CNTs is presented. The thesis ends with the overview report of fabrication.

1 Theory

1.1 Bolometer Definition and Infrared Detectors Classification

The word bolometer is originated from Greek language, and it literally means a ray-meter [1]. Infrared (IR) detectors may be classified into the two main groups: photon detectors and thermal detectors [2].

The photon detectors have to be cooled down almost to temperature of liquid nitrogen (63–72) K, therefore there is a need for cool down systems. This sort of cool down system is the most expensive part in a conventional photon detectors' IR camera. On the other hand, most of thermal IR detectors were fabricated without such an apparatus. These types of systems are called uncooled and are inexpensive compared to photon detectors [3]. Bolometers are thermal infrared function sensors absorbing the incident radiation energy which changes the bolometer temperature. The temperature increase is dependent on incident infrared flux, and is measured with the thermocouples, pyroelectric, resistive, ferroelectric, and other temperature sensing principles. The term “infrared bolometer” commonly refers to resistive microbolometers in the uncooled IR imaging technologies. In the resistive microbolometers, the temperature increase is measured by resistance change [4,5].

Uncooled IR bolometers have become the main and dominating technology for the majority of commercial and military IR imaging applications. The most common IR imaging applications are thermography, night vision (namely military, commercial, and automotive), reconnaissance, surveillance, firefighting, medical imaging, predictive maintenance, and industrial process control [4].

Nowadays, the common understanding of bolometer term refers to the thermistor bolometer. It is temperature-variable resistor. By measuring the change in the resistance, it is possible to find a signal which is dependent only on the bolometer experiences due to incident IR flux.

1.2 Brief History of Bolometer and Infrared Detectors

The IR radiation had been unknown until 200 years ago when Herschnel's experiment with thermometer was reported in April 1800. This thermometer was a crude monochromator which used thermometer as a detector so the energy distribution in sunlight could be measured. The Fig. 1.1 shows the milestones of IR detectors development. In 1829, Nobii constructed the first thermophile by connecting a number of thermocouples in series. In 1933, Melloni modified thermocouple design by using bismuth and antimony for it. Another step was the appearance of

Langley's bolometer in 1880. Two thin platinum foil ribbons were connected as two arms of Wheatstone bridge in the bolometer. Langley continued to develop his bolometers for following 20 years, and his later devices were 200 times more sensitive than his first devices. The Langley's last bolometer was able to measure the heat from a cow at distance of a quarter of mile, so that is considered as the milestone in the development of IR detectors connected with thermal detectors. The thermoelectric effect was discovered by Seebeck in 1921, and soon thereafter he demonstrated the first thermocouple which was very important step in IR detection development [2,6,7].

In history, there have been investigated many materials in the IR field, and many physical phenomena have been proposed for IR detection. The important physical principles used in the development of IR detection are thermo-electric power (thermocouples), change in electrical conductivity (bolometer), gas expansion (Golay cell), pyroelectricity (pyro detectors), photon drag, Josephson effect (Josephson junction), internal emission (PtSi Schottky barriers), fundamental absorption (intrinsic photo-detectors), impurity absorption (extrinsic photodetectors), low-dimensional solids (super lattice and quantum well detectors), different type of phase transition, etc.

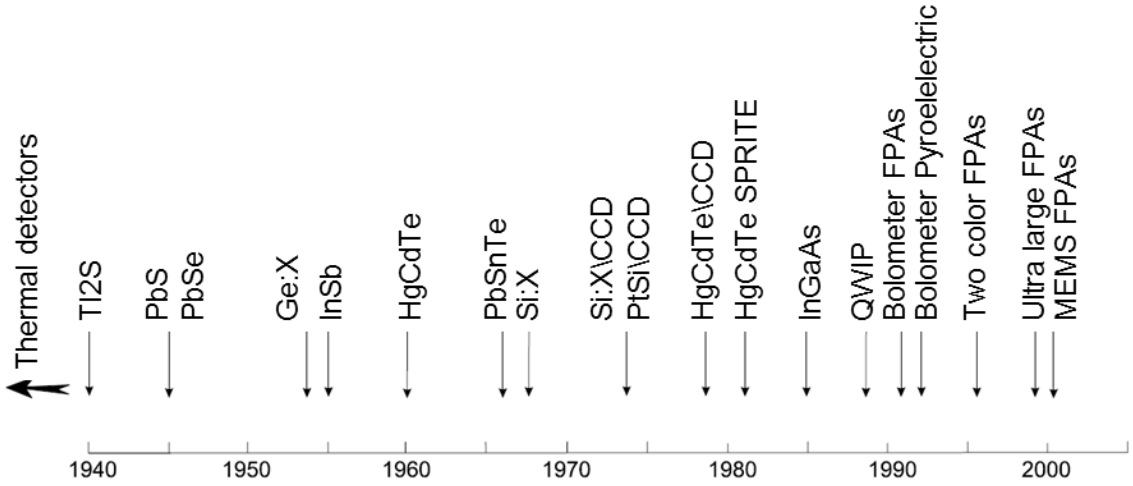

Fig. 1.1 History of IR detectors development [2]

The origin of modern IR detector technology was seen during the World War II. The wavelength of two atmospheric windows in the range of (3–5) μm and (8–14) μm has been interesting for continuing progress though for space application, there has been an increasing interest in longer wavelength [2].

The resistive thin film bolometer has been proposed from 1947 to 1980. Honeywell has been publishing its development of the uncooled IR microbolometers and focal plane array technology since late 80's [4].

The requirements for future application of IR detector are:

- higher pixel sensitivity, further increase in pixel density to above 10^6,
- cost reduction in IR imaging array systems through the use of less cooling sensors technology combined with integration of detector signal processing function (with much more on-chip signal processing),
- improvement in the functionality of IR imaging through development of multispectral sensors [2].

1.3 Basic Physics Terminology for Thermal Engineering

1.3.1 Heat Transfer

Heat transfer is provided via three modes; conduction, convention, and radiation. Conduction is more proceeded in solids and based on molecular diffusion caused by temperature gradient. There is not a complete understanding of radiation mechanism. Heat transfer due to radiation mechanism appears in solids, liquids, and gases. On the contrary, convention is solely because of the fluid bulk motion, transferring heat in the process. Thereby, convention heat transfer is applied only on fluids. The constitutive relation in heat conduction, heat convention, and thermal radiation is known as Fourier's law, Newton's law of cooling, and the Stefan-Boltzmann law, respectively [8].

1.3.2 Thermal Conduction

As noted above, heat conduction is transfer of heat energy proceeded by diffusion and microscopic particles collision due to existing temperature gradient. The diffusing particles (molecules, electrons, atoms) transfer disorganized kinetic and potential energy. Conduction is possible only within an object or material, or between two objects which are in direct or indirect contact with each other [9]. Consider a slab of face area *A* and thickness *L*, whose each face has different temperatures T_H and T_C by hot reservoir and cold reservoir. The q is the heat flux, defined as the heat flow *Q* per unit area *A* and time *t.* Thus, Fourier law of heat conduction, the heat flux in the slab may be expressed as:

$$q = \frac{Q}{At} = G\frac{T_H - T_C}{L}, \qquad (1.1)$$

in which *G*, called the thermal conductivity, is material property constant [9,10].

Thermal conductivity *G*, as a transport property of material, is the proportionality factor between the rate of heat flux *Q* and the temperature gradient with respect to distance;

$$\frac{\dot{Q}}{A} = -G\frac{dT}{dx}, \qquad (1.2)$$

where the *A* is the area face of slab.

Thermal capacity, a thermodynamic property of a substance is defined as constant as the material density ρ and specific heat *c*. Thermal capacity *H* is energy storage ability of a substance and can be calculated from the following equation:

$$\mathrm{Q} = H(T_i - T_f), \qquad (1.3)$$

in which T_i and T_f are incipient and final temperatures, respectively [9].

1.3.3 Thermal Radiation

Thermal radiation is the most interesting mode of heat transfer for bolometer applications. The thermal radiation does not require a material medium. It all began with classical mechanics explaining the waves based on Maxwell's equations. Logically, the most challenging task was discovering and describing the nature of light which was thought to behave only as a wave. There was a paradox, though, how can a wave travel in the empty space. It was the development of quantum physics which made possible description of particles and waves as two distinct modes of behavior. The wavelength is defined for particles in the field of quantum physics. Max Planck expressed energy of particle as electromagnetic radiation in terms of wave frequency [8].

The thermal radiation is radiation emitted as a result of the object temperature. The object surface is either emitting or receiving radiant energy. The radiant power (the rate of emission energy via electromagnetic waves) is defined by following equation:

$$P_{rad} = A\varepsilon\sigma(T^4 - T_0^4), \qquad (1.4)$$

where T_0 is the ambient temperature, *A* is the radiant surface, ε is the emissivity, and σ is the Stefan-Boltzmann constant, namely $\sigma = 5.67\times10^{-8}$ W/(m^2.K^4) [9].

Infrared radiation is part of electromagnetic spectrum with wavelength in the range of (0.75–1000) μm. The transmission of IR allowed by the atmosphere is in the (3–5) μm and in the (8–14) μm wavelength regions. Black body with temperature of 300 K has intensity peak of emitted radiation of about 10 μm. The radiation flux from real objects has different values depending on the surface emissivity of the object [4].

1.3.4 The Heat Transfer Equation

The heat transfer equation states the incident power $P_{incident}$ equals the thermal conductance G times the change in temperature, plus the thermal capacity H times the rate of temperature difference. This equation is a statement of energy conservation [5,11]:

$$P_{incident} = G\Delta T + H\frac{d\Delta T}{dt}. \tag{1.5}$$

1.4 Bolometer Physics

This chapter describes fundamental bolometer physics. In the beginning, the thermal detectors are described following by the bolometer operation, which is to be proposed and fabricated.

1.4.1 Thermal Detectors

As mentioned previously, the thermal detectors are classified regarding to their basic operation principle; thermopile, bolometer, thermomechanical or pyroelectric. The scheme of general thermal detector can be seen in Fig. 1.2. The detector element is connected by two conductive paths to the heat sink. In case, the radiation is incident on the detector, the temperature change is determined by equation (neglecting the radiation heat loss) [2]:

$$H\frac{d\Delta T}{dt} + \mathrm{G}\Delta\mathrm{T} = \varepsilon\Phi, \tag{1.6}$$

where H is the thermal capacitance, G is the thermal conductance, ΔT is the temperature difference due to incident radiation Φ between the detector and its surroundings, and ε is the detector emissivity.

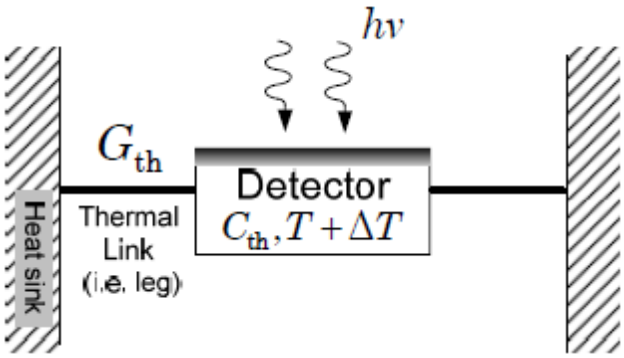

Fig. 1.2 Detector element connected by two conductive paths to heat sink[12]

The temperature in the detector structure is increasing due to incident IR radiation, therefore the physical or electrical property of the temperature-dependent detector is changing. There is a response speed limit. The value of temperature difference is dependent on thermal capacitance, thermal conductance, and substance mass. In order to achieve a fast response, there is a common way to minimalize substance mass. Hence, the suspended membrane is very common design structure for IR detectors [5,12,13].

1.4.2 Thermal Detection of Uncooled Bolometer

As mentioned before, the bolometer is a device whose electrical resistance changes as function of its temperature. Resistive change ΔR_b dependent on temperature change ΔT is described in equation bellow:

$$\Delta R_b = \alpha R b \Delta T, \tag{1.7}$$

where α is the temperature coefficient of resistance TCR that is defined as:

$$\alpha = \frac{1}{R_b}\frac{dR_b}{dT}. \tag{1.8}$$

1.4.3 Bolometer Physical Description

In this section, there is useful description of some bolometer parameters which are important for the final chip fabrication, and for following read-out circuit design, as well. The physical parameters including material properties are regarding to one pixel. Consider IR radiation is incident on the sensing area and heats up the structure in consequence. There is a need to achieve the high ΔT so the thermal conductance G between the bolometer structure and the thermal sink, in MEMS technology the silicon wafer, has to be minimized. Time constant τ_{th} is an important parameter for bolometer design, and it is defined as:

$$\tau_{th} = \frac{H}{G}, \tag{1.9}$$

where H is the thermal capacitance of bolometer structure. This thermal time constant equation determines the response rate of thermal detector. In case, the bolometer structure has high thermal capacitance value, it is clear the response of thermal change is slow. The time constant is important for cooling down the structure as well as to define the frequency of measurement repeating [12,14].

1.4.4 The Self Heating Effect of Bolometer

The bolometer temperature is changing due to incident IR radiation and more significantly due to the Joule heating or self-heating. Consider a supply voltage which is applied to the bolometer for measurement. This supply voltage heats up the sensor by power in the milliwatts

range compared to the incident IR which heats up the sensor by power in the nanowatts range. According to the differential heat balance equation, the self-heating steady state power P_{SH} dissipated due to applied *dc* bias V_{dc} can be expressed by:

$$P_{SH} = \frac{V_{dc}^2}{4R_0}, \tag{1.10}$$

where R_0 is the resistance of bolometer according to ambient temperature [15]. Solving the heat balance equation, it is possible to define ΔT following time dependence [16]:

$$\Delta T = \frac{V_B^2}{4GR_0}\left[1 - exp\left(-\frac{t}{\tau_{th}}\right)\right] + \frac{P_s}{G}, \tag{1.11}$$

where V_B is the voltage pulse during measurement, G is the thermal conductance, τ_{th} is the thermal time constant, and R_o is ambient temperature resistance [17].

1.4.5 Bolometer System Noise

The noise definition is described as any unwanted signal component. Unfortunately, the micro bolometers are significantly affected by different types of noise. The micro bolometer noise is categorized as background noise, detector noise, and the readout noise. The detector noise is major for bolometer structure, and the noise sources are temperature fluctuations, Johnson noise, and flicker noise. The background fluctuation is necessary to deal with during the bolometer design. The background fluctuation is not a dominant factor of total noise but it puts the limit of detector performance. It is predicted to be totally random in nature.

Detector temperature fluctuation noise is the other type of noise source in micro bolometer. The bolometer simply represents the temperature dependent resistance as shown above; therefore a temperature fluctuation is immediately transformed into the output noise. **Johnson noise** is one of the most representing noise sources. In the bolometer metal electrode, it is basically the only significant contributor of noise since the flicker noise is usually very less. **Flicker noise** is low frequency type of noise, appearing simply due to non-ideal conditions of material surface, and the layers interface. The type of noise is a very limiting parameter mainly for semiconductor bolometers, which have high resistance in the range of mega ohms [18].

1.5 Bolometer Design

1.5.1 Bolometer Chip

The bolometer design is fundamental stage in the bolometer fabrication. There are numerous of design features and trade-offs which have to be considered as mentioned above. The low thermal conductance between bolometer and its surrounding, the high absorption of the IR

radiation including the option of a sensing material with high temperature coefficient of resistance, and low 1/f noise properties, and as low thermal time constant as possible, these are the most important parameters which have to be considered during the bolometer design. Nowadays, the typical size of a commercial pixel is about 17 μm × 17 μm. These sorts of pixels allow achieving the focal plane of high resolution arrays at acceptable cost [4].

The typical bolometer design is shown in Fig. 1.3. Small thermal conductance between bolometer and its surroundings is obtained by using the long bolometer legs. The low thermal capacity is achieved by small cross section area using the materials with low thermal conductivity. There is a metal electrode on the legs which provides the contact between the IR detecting material and the read-out circuit. The modern bolometers have thermal conductivity between legs and substrate typically as low as 3.5×10^{-8} W/K. There is a need to minimize the thermal convection between the bolometer and its surroundings so the conventional bolometer chips are in vacuum package with pressure in the order of 0.01 mbar (1 Pa) [4,5].

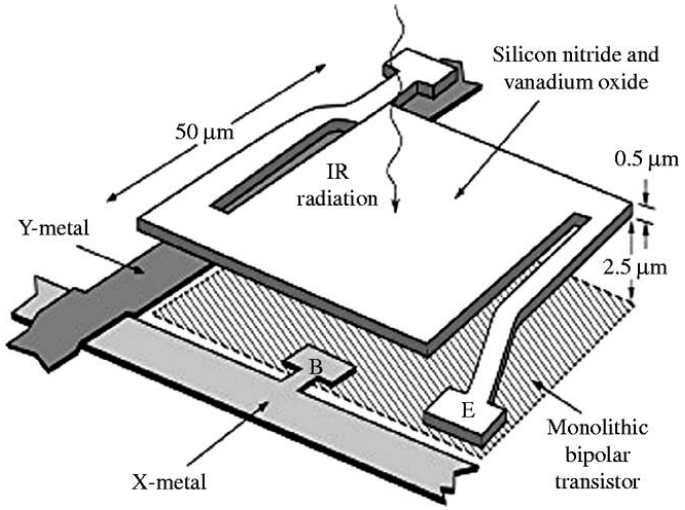

Fig. 1.3 The typical bolometer structure [12]

1.5.2 Focal Plane Arrays

The focal plane arrays (FPAs) are the ordering or placing principle of single bolometer chips. The FPAs typically consist of two dimensional matrixes to create a focusing IR detection system. The IR FPAs are fundamental and key part of modern advanced IR imaging systems. There are number of architectures used for IR detection devices. In general term, there is a classification of FPAs as monolithic and hybrid. Considering the monolithic approach, there is no external read-out circuit, so the multiplexing is proceeded in the detector itself. The basic structure for monolithic FPAs is a metal on insulator (MIS) structure. On the other hand, the hybrid FPAs detectors and read-out circuits are fabricated on different substrates and connected to each other employing the flip on chip bonding technique or loop-hole interconnection. The advantage of

such ordering is an option of optimizing the detector material and read-out circuit independently [2,4,12].

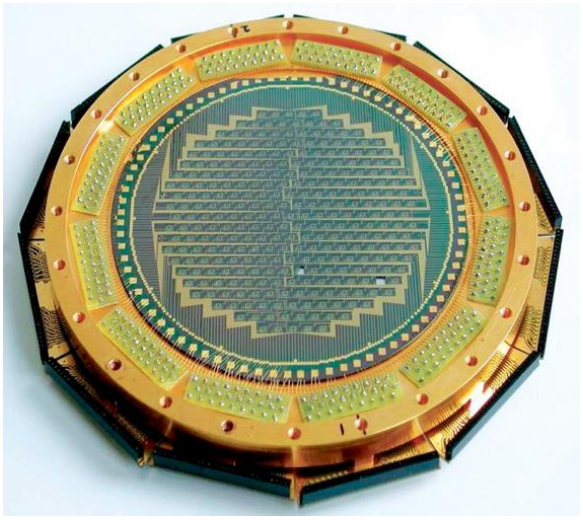

Fig. 1.4 The LABOCA FPA design of the multi-channel bolometer [19]

The Fig. 1.4 shows the image of LABOCA which is the modern FPA developed in the Max-Planck Institute for radio astronomy. LABOCA is the multi-channel bolometer array for continuum observation mode and it operates in the 870 μm atmospheric window. The signal photon flux is absorbed by a thin metal layer cooled to about 280 mK. This array consists of 295 channels in 9 concentric hexagons [19].

1.5.3 Bolometer Temperature Sensing Materials

The temperature sensing material is one the most important issues to obtain the high sensitive IR detector. The suitable material for such application has to have high temperature coefficient of resistance (TCR), and low 1/f noise value. Considering the common commercial applications, the sensing material has to be compatible for integration to read-out circuits. Today, the most used materials are vanadium oxide (VO_x), amorphous silicon (α-Si), and silicon diodes. The vanadium oxide films used to have the TCR in the range of 2 %/K and 3 %/K at room temperature. Today, the bolometer characteristics using this layer can be improved by employing the vanadium-tungsten oxide made by low temperature oxidation of vanadium-tungsten metal films. Another effect on the layers has been achieved by using the reactive pulsed deposition for Ti-W layer, and today, it is possible to obtain a VO_x layers with TCR of 5.12 %/K. The VO_x film is the most used in present bolometer products [2,4,20].

The amorphous silicon (α-Si) is also applied in numerous bolometer devices. The α-Si microbolometer arrays have advantage of complete compatibility to silicon fabrication technology, high optical absorption and TCR is up to about 3 %/K. The bolometer made of α-Si

commonly consists of thin suspended membrane which leads to low thermal time constant, and low thermal conductivity. The α-Si based bolometer arrays are cheaper to fabricate for high volume application [2,4,20].

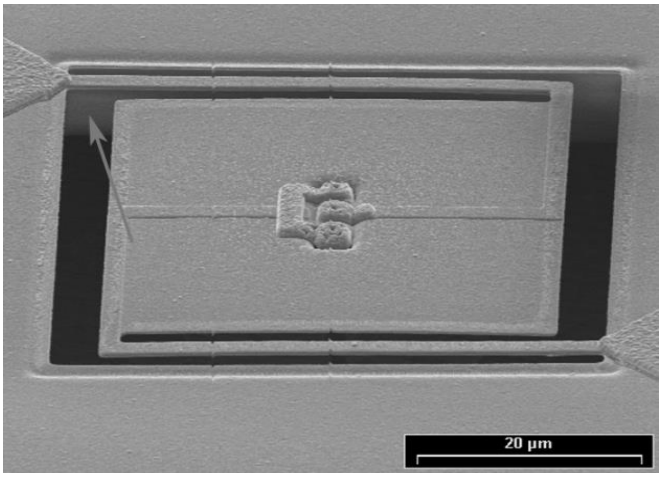

Fig. 1.5 The semiconductor diode bolometer [21]

There have been many attempts to replace the resistive temperature sensors with semiconductor diode made of single-crystal for its stability and the low value of the noise (shown in Fig. 1.5). Diode has an advantage of multi modes running, it can operate as constant current or constant voltage even at the biased or reverse biased. The most challenging issue is the thermal isolation of this structure [21].

1.6 Read-Out Circuit

The read outs circuits for bolometers have to measure the low resistance change of individual bolometers. As mentioned before, there is also relatively high value of noise sources in the bolometer detector, and the read-out circuit noise. The bias voltage is necessary for measuring the resistance change, though the voltage causes the self-heating effect, so the read-out circuit is required to handle higher dynamic range. In the commercial FPA's, the column parallel read-out architectures with integrated AD conversion are commonly employed [4].

1.6.1 Read-Out Circuit Using a Wheatstone Bridge

The Wheatstone bridge has been known since 19^{th} century and it is not common way to read the resistance change in modern IR detector applications. As it will be discussed later, it is very useful and simple tool to investigate the bolometer chip behavior for this thesis purpose. The simply read-out circuit, using the Wheatstone bridge, is shown in Fig. 1.6. The bolometer B_1 is exposed to IR radiation and the bolometer B_2 are covered with the reflection layer so the IR flux would not change its temperature [5,17,22].

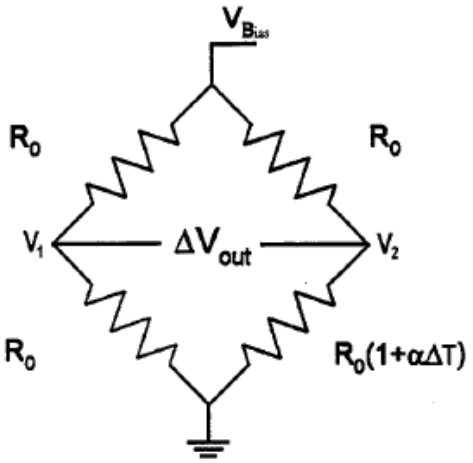

Fig. 1.6 Wheatstone bridge with one bolometer (temperature dependent resistor) [5]

The Wheatstone bridge can be seen as two voltage dividers considering there is no flowing current in the node connecting V_1 and V_2. The voltage signal V_{OUT} as a function of temperature is described as:

$$V_{OUT} = V_s \left[\frac{\alpha \Delta T}{4}\right], \tag{1.12}$$

where α is the temperature coefficient of resistance and V_s is the supply voltage applied during the measurement [5].

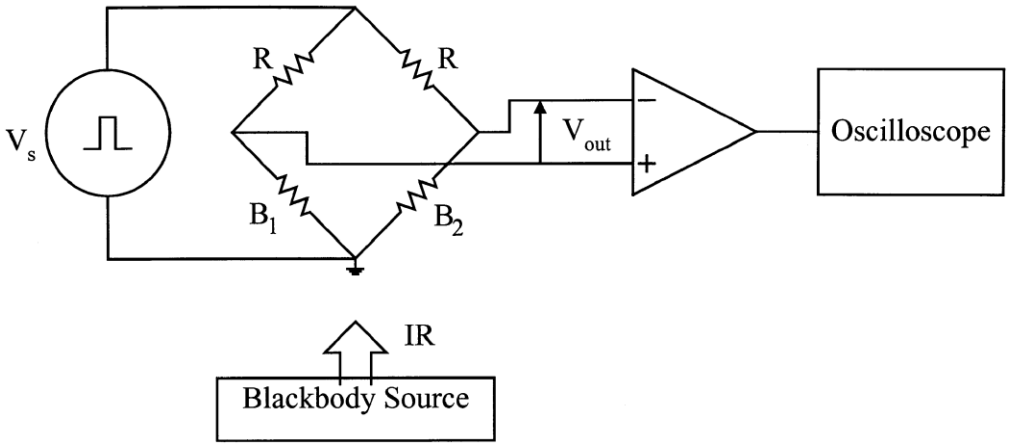

Fig. 1.7 Wheatstone bridge circuit and test setup used for the study of self-heating compensation [16]

Fig. 1.7 shows the Wheatstone bridge with two fixed resistors R_1, R_2 and B_1,B_2 are two microbolometers with specific thermal parameters. Considering the heat balance equation in which the self-heating effect is included, the heat balance equation is now:

$$H\frac{d\Delta T}{dt} + G\Delta T = P_{SH} + \Phi, \tag{1.13}$$

where H is the thermal capacity, ΔT is the temperature change of microbolometer with respect to the heat sink, G is the thermal capacity of the detector structure, P_{SH} is the power dissipated due to self-heating effect, Φ is the incident IR flux power [23]. Considering that for $\alpha\Delta T \ll 2$, where α is the thermal coefficient of resistance (TCR), the equation for V_{OUT} is described as:

$$V_{OUT} = \frac{V_S^3}{16R}\left[\frac{\left(1-e^{t/\tau}\right)}{G}\right] + \frac{V_S \alpha \Phi}{4R}\left[\frac{1}{G}\right]. \quad (1.14)$$

The Fig. 1.8 shows the time dependence of temperature change. It is representing the applied voltage pulse and the cooling time.

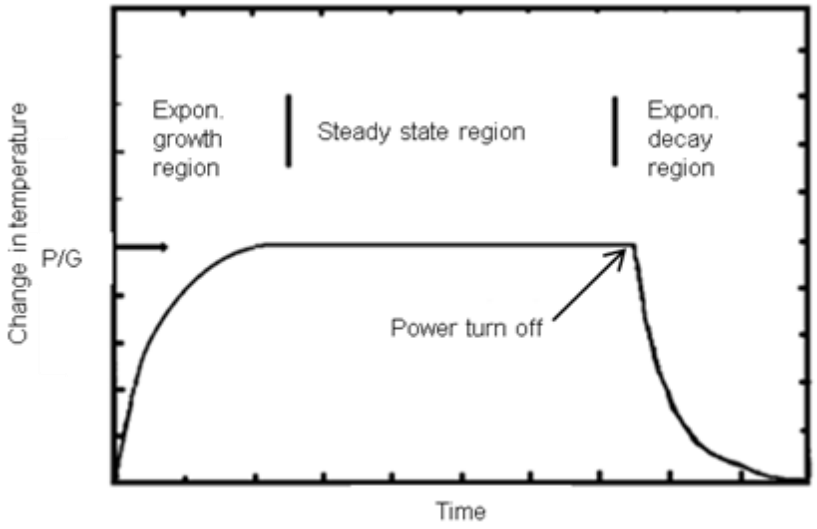

Fig. 1.8 Thermal detector step response of temperature change

In the case the Wheatstone bridge is used for measurement of real bolometer sample, the bolometer is exposed for a more than three times constant in order to achieve steady state, applying the supply voltage pulse, and then measures the output voltage [5,23]. Considering one bolometer is exposed and the reference is covered by reflection layer, the output voltage would be as it is shown in Fig. 1.9 bellow. This figure shows the difference between exposed and covered bolometer but is only for illustrative purpose. Truly, it is a gross exaggeration due to six orders differences between the incident IR flux power and the self-heating power. If the supply voltage would not be removed, the amplifier would cause the quick saturation and probably the damage of the whole structure [5,17].

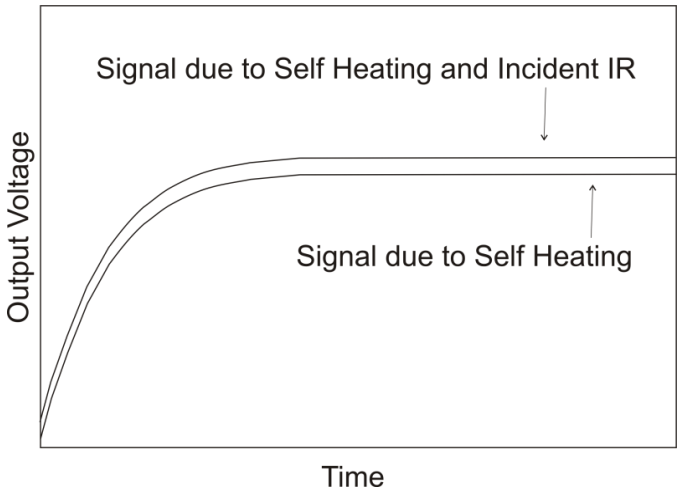

Fig. 1.9 Exaggerated illustration of the output voltage due to self-heating effect alone, and self-heating effect combined with the incident IR radiation [5]

2 Absorption Layer Characterization

The absorption layer is one of the key parameters for IR detection devices. The most used materials are vanadium oxide (VO_x), amorphous silicon (α-Si), and silicon diodes as mentioned in the theoretical part of this work. In this thesis, carbon nanotubes CNTs layer is applied for detection of IR in order to explore new possibilities and to improve the structure sensitivity.

In this chapter, the fabrication process and characterization of CNTs layer is described. The Fourier transform infrared spectroscopy FT-IR is performed to determine the absorption of CNT's.

2.1 Theory of FT-IR Measurement

The FT-IR is one of the most used methods of infrared spectroscopy [24]. The method could be simply described as an absorption measurement with the different IR frequencies of a sample placed in the path of IR beam [25]. The absorption in the IR region results in changes of vibrational and rotational status of the molecules. The absorption intensity depends on the IR photon energy which can be transferred to the molecule and this depends on the change of the dipole moment that occurs as a result of molecular vibration. As a consequence, a particle (namely molecule] will absorb the IR light only if the absorption causes a change in the dipole moment. The absorption frequency is dependent on the vibrational frequency of the molecule[26].

2.1.1 Principle of ATR Method

The ATR is the abbreviation of attenuated total reflection. The principle of this method is measuring the changes in a totally internally reflected IR beam in the case the beam comes into contact with measured sample. The IR beam is directed on the optically dense crystal with high refractive index at a certain angle. The method requires the sample is in the direct contact with the ATR crystal because the evanescent wave only extends beyond the crystal in the range of 0.5 μm–5 μm. The refractive index of the crystal must be greater than the index of crystal [25].

2.1.2 Principle of Transmission Spectroscopy Method

Transmission spectroscopy method is the oldest and probably the most straightforward IR method. The basic principle is based upon the IR absorption at a specific wavelength as it passes through the sample. This method is traditionally preferred to spectral interpretation. It is possible to analyze the matter in three forms: solid, liquid or gaseous [26].

2.2 Deposition of CNTs Layer

The final bolometer chip is employing the vertically aligned CNTs deposition on the chip itself. In case of elementary measurement to characterize the absorption layer, the CNTs have been deposited using chemical vapor deposition CVD. The deposition process for measured samples is as follows. As the substrate, the silicon wafer with orientation 100 and thermal silicon dioxide layer with thickness of 0.5 μm is used. The cobalt film with thickness of 5 nm serves as catalytic layer. The thickness of the catalytic material is related to the CNTs diameter. During evaporation, the deposition rate is 0.01 nm/s in order to obtain a homogenous layer and to minimize grain size. The evaporation is applied using a template to create CNTs selectively in the area similar to the desired area on the chip.

The CVD deposition is setup with parameters described below. The heating up to the temperature for CNT growing is done in the argon atmosphere with flow of 1400 sccm. When the temperature is reached, there is a time period of 15 min when the argon (1400 sccm), the nitrogen (50 sccm) and the acetylene (58 sccm) are applied on the sample. The cooling down time period is 2 hours with Ar gas flow of 1400 sccm to reach the temperature bellow 200 °C. The growing temperature is different for precise sample. The sample denoted hereafter CNT221 is prepared at the growing temperature of 650 °C, CNT231 at 600 °C, and CNT232 at 600 °C as well.

The grown CNT is shown in the Fig. 2.1 It is obvious their structure does not perfectly corresponds to nanotubes but rather to the carbon nanowires could be the term for this type of structure. There is a number of defects and the CNTs are mostly twisted. Nevertheless, for FT-IR measurement and the following IR characterization these samples are suitable.

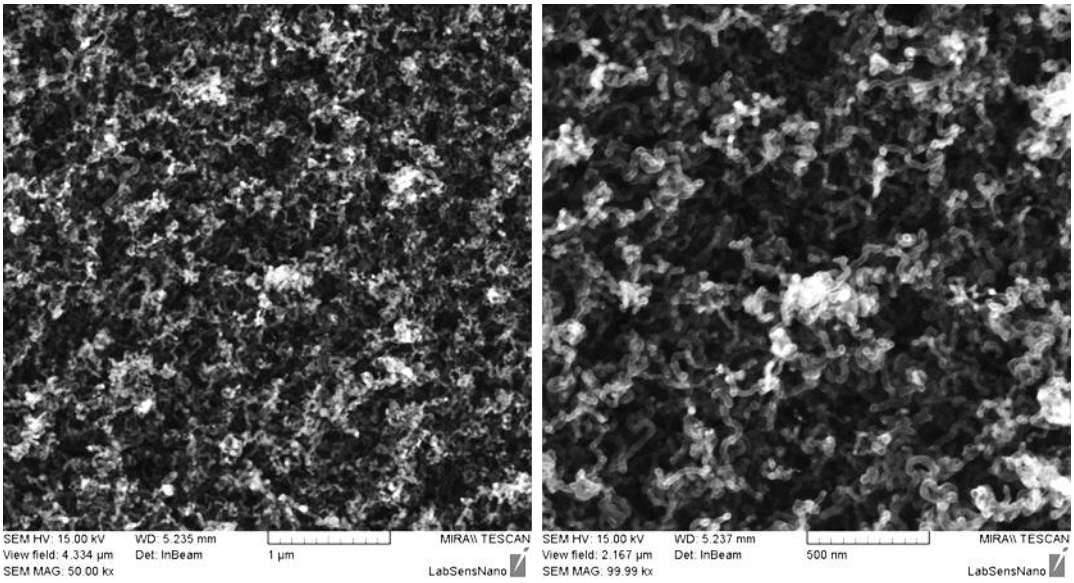

Fig. 2.1 SEM image deposited CNT's

2.3 FT-IR Measurement Results and Discussion

The IR spectra have been recorded using FT–IR spectrometer Nicolet iS50. Both the ATR method and the transmission are employed to compare the results. The measurement procedure is performed for silicon substrate with the thermal oxide of 500 nm thickness in the first case. The Co layer on the same substrate is then measured, and finally the samples with grown nanotubes structures to determine the efficiency of an applying the CNT in the IR detection.

The Fig. 2.2 shows the results of the ATR FT-IR measurement. The measurement is performed for the wavelength 2.5–22.5 μm. There is a significant difference of IR absorbance for substrate without (SiO_2, Co_layer) or with the grown CNT (CNT 231, CNT 232, CNT 221). The interval from 2.5 μm to 7.5 μm clearly represents the absorbance of substrate. The local low points of the curve in the approximately 9.0 μm shows the typical progression for the atmospheric humidity. The absorbance of the CNT is mostly seen in the interval form 8 μm to 22 μm. In case the absorbance value is higher than 1.0 it is caused by an inaccuracy of the measurement. As mentioned before, the main interest is 8–14 μm in the range of wavelength spectrum due to so called atmospheric window.

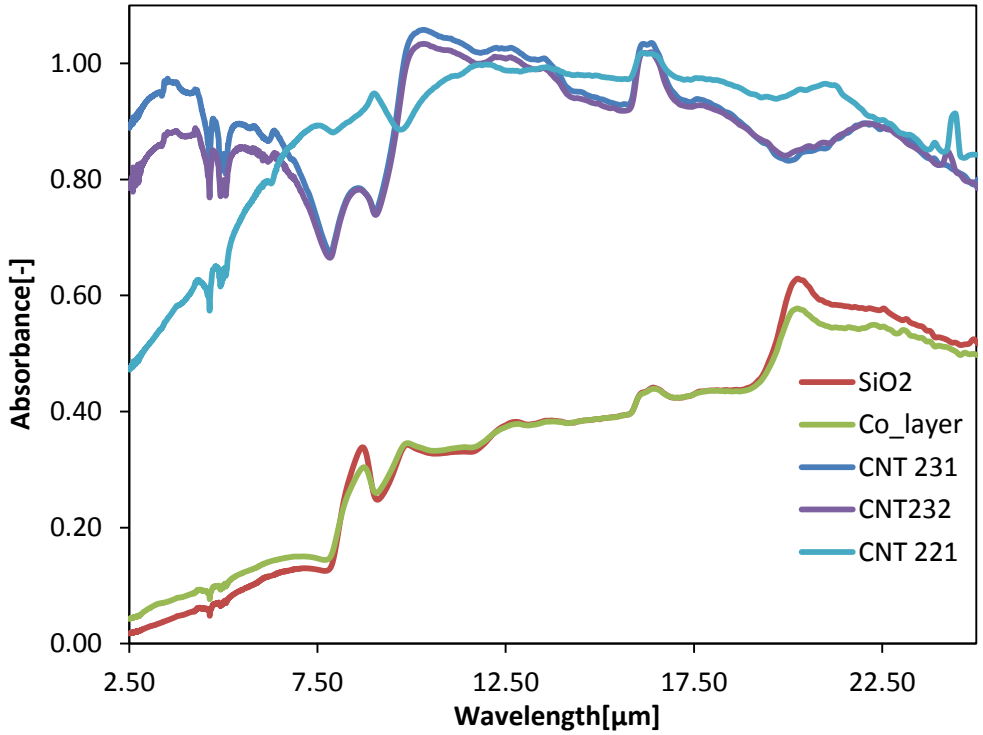

Fig. 2.2 ATR FT-IR plots represent the comparing of samples

The transmission method is performed to avoid the serious measurement errors. Consequently, it confirms the previous results of the absorbance and proves the CNTs layer will significantly improve the IR detection of bolometer.

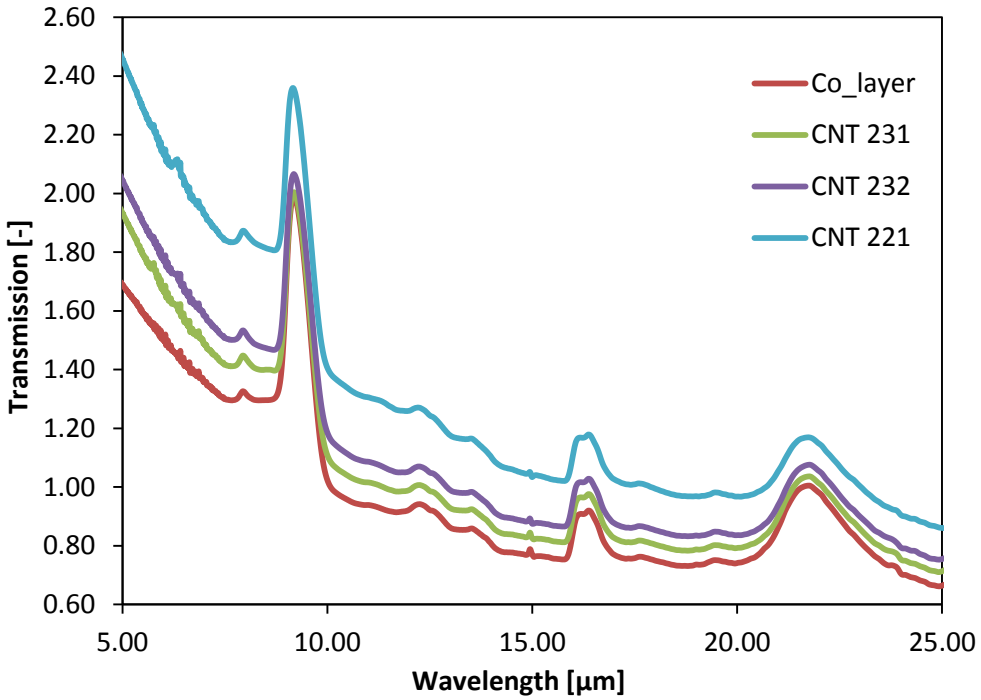

Fig. 2.3 Transmission study of IR

The efficiency of CNTs is confirmed by this measurement. From the physical principle of the material absorption it has been well known the particle dipole moment is necessary. No modification for CNTs to create the dipole moment is required according to the FT-IR results. The measured absorption confirms the critical parameter is the absorption near to 100 %. Concluding from above mentioned, the usage of the CNTs deposition on the chip is a new technological process which should improve sensitivity of the bolometer device.. Therefore, it is important to realize the absorption of this whole layer is dependent on the diameter and the density of vertically aligned CNTs and further it is necessary to optimize the process CNTs fabrication on the chip.

3 Design of Bolometer Chip

The design of bolometer chip has been done using Cadence 5.1.4 Software. Hierarchical design is necessary part as well as setup of parametric cells. There are 6 masks for lithography process. The contact lithography technique is used so the maximum resolution is 2.2 μm. The GDSII steam (Graphic Database System) file is to be exported for following bolometer fabrication. The file is industry standard for data exchange of integrated circuit or IC layout artwork. The data in GDSII format are in the binary code representing planar geometry shapes, text labels, and other information about the layout in hierarchical code [27].

3.1 Description of Bolometer Design Cells

The bolometer structure is to be as suspended membrane which is quite a conventional design. The complete fabrication process plan with all materials' overview will be described in the chapter 4 and the chapter 6. There are six types of bolometer array cells, each meant for specify measurement or bolometer material properties deriving. Each array cell is with size (3×3) mm, one of these is shown in Fig. 3.1, the cross design has been used except the serial parallel bolometer combination which is in different designed array, of course. The chip is with size 1.5×1.5 cm and it consists of 25 bolometer arrays. The detail description of arrays and bolometer structures are following.

3.1.1 The Van der Pauw resistivity structure

The Van der Pauw resistivity structure is commonly used for microtechnology process monitoring or the thin layer characterization, the cell is shown in the Fig. 3.1. Specified resistivity or Hall Effect of arbitrarily shaped disk could be measured. There are some necessary conditions which have to be respected in order for this technique to work. The structure has to be of uniform thickness, be homogenous in the composition, and be symmetrical. The contacts have to be on the perimeter of the structure and they need to be much smaller than the area of the structure. According to the met condition, following relation states [28]:

$$e^{-\left(\pi\frac{d+R_{AB,CD}}{\rho}\right)} + e^{-\left(\pi\frac{d+R_{BC,AD}}{\rho}\right)} = 1, \qquad (3.1)$$

where the $R_{AB,CD}$ is the resistance of the structure when current is flown through input A and output B contacts according to the Fig. 3.1. The voltage is measured across the C–D contacts. The $R_{BC,AD}$ is the resistance when current is flown through input C contact and output D contact. The voltage is measured across the contact A–D. The thickness of structure layer is d, and ρ is the resistivity of the layer material.

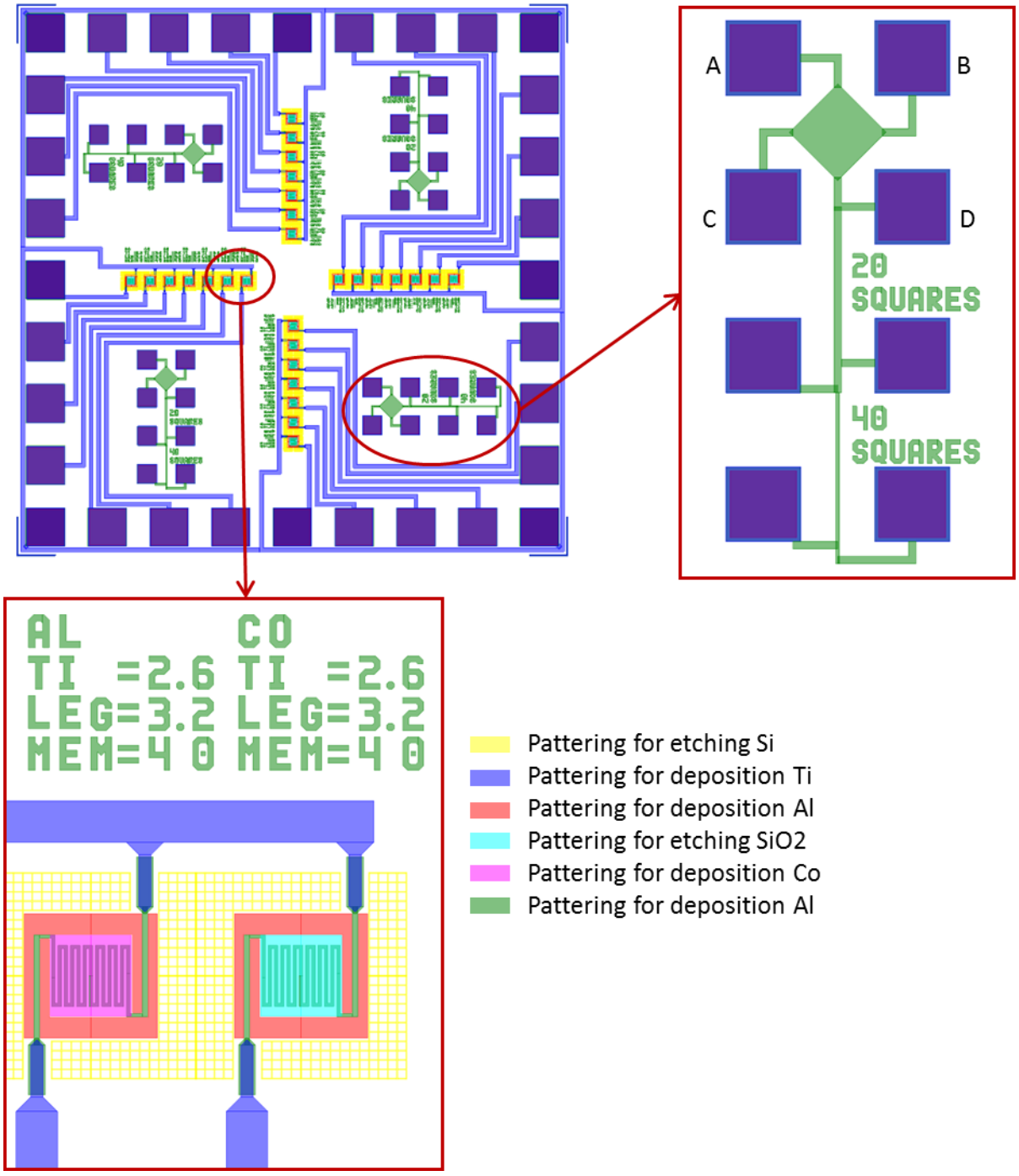

Fig. 3.1 Bolometer chip (cross ordering), detail of Van der Pauw structure for sheet resistance measurement, and detail of bolometer structure design

Considering the Van der Pauw structure cell of bolometer design, the sheet resistance R_S (Ω/□) can be calculated as:

$$R_S = \frac{\pi R}{\ln(2)}, \tag{3.2}$$

where the R is the measured resistance as it has been previously described.

3.1.2 Single Bolometer Cell

The single bolometer cell is shown in the Fig. 3.1. Purpose of each layer (mask) will be described in the fabrication process chapter no. 6. The bolometer cell detail shows the masks for bolometer structure, and there are informative signs made of aluminum (green color) so it is absolutely clear what type of structure is dealt with. The sign Al/Co (shown in Fig. 3.1) says if there is a cobalt layer for carbon nanotubes deposition to absorb the IR, or there is aluminium layer on the membrane as a reflection layer. The sign (*Ti = 2.6*) states the width of titanium electrode; in this case it is 2.6 μm. The leg sign (*LEG = 3.2*) says the thickness of membrane legs in micrometers. The sign most bellow (*MEM = 40*) says the size of suspended membrane which is the (40×40) μm square shape.

3.1.3 Cell for Measurement of Titanium Layer Material Properties

The titanium electrode embedded in the bolometer structure has tremendous meaning for desired measurement. It is titanium resistance which is detected during bolometer operation. Therefore, it is very important to determine the material properties. The R_0 value is the value of electrode measurement at ambient temperature. As shown in Fig. 3.2 the width of Ti electrode is changing in range of (1.6–3.6) μm to determine if there is any affectation on major thermal parameters of bolometer chip.

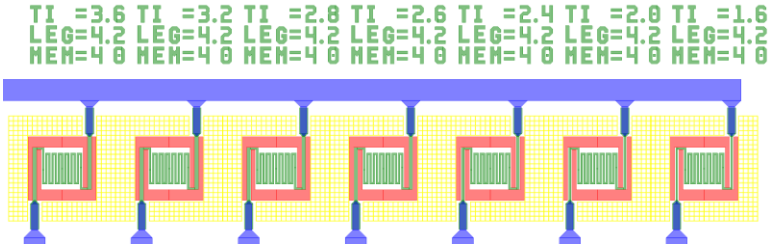

Fig. 3.2 Detail of cell for measurement of Ti layer materials properties

3.1.4 Cell for SiO_2 Thermal Conductance Measurement

Thermal conductance *G*, thermal capacitance *H*, and the thermal time constant are the fundamental, major parameters for bolometer structure, and it is important to determine these materials properties. The bolometer chips consist of several cell types for these kinds of

measurements. The parametric cell with variable leg width in the range of (2.2–4.2) μm is shown in Fig. 3.3.

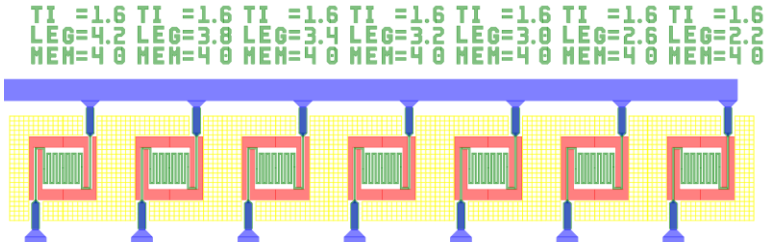

Fig. 3.3 Cell for SiO_2 thermal conductance measurement.

The measurement setup is reported in reference [17]. The basic principle is related to the heat balance equation. Using the equation for ΔV_{OUT}, the difference between two measurement of single bolometer chip can be derived with and without applying dc bias which provides the value of thermal conductance G.

$$\Delta V_{PS} = \frac{\alpha V_B V_{DC}^2}{16 \Delta V_{PS} R_0 G}, \tag{3.3}$$

where

$$\Delta V_{PS} = \Delta V_{OUT(DC=PS)} - \Delta V_{OUT(DC=0)}. \tag{3.4}$$

The variables in both equations are ΔV_{PS} which is the difference between measurements with and without applying of bias dc offset, α is thermal coefficient of resistance, V_B is the amplitude of bias pulse voltage, V_{DC} is the value of dc offset of bias pulse voltage, and R_0 is the bolometer resistance at ambient temperature [15,17].

In order to determine the value of bolometer thermal conductance, there is constant voltage pulse while the value of V_{DC} is variable. The bridge differential voltage is then function of applied V_{DC} (shown in Fig. 3.4), it is obvious the curve is nonlinear. The nonlinear curve is fitted according to the polynomial function of second order. According to this, the results are equal to the value of the bolometer thermal conductance [15]. The reason there are single bolometer chips with different leg widths (different values of G) is to make the measurement as much precise as possible, and it is very useful to eliminate the measurement errors.

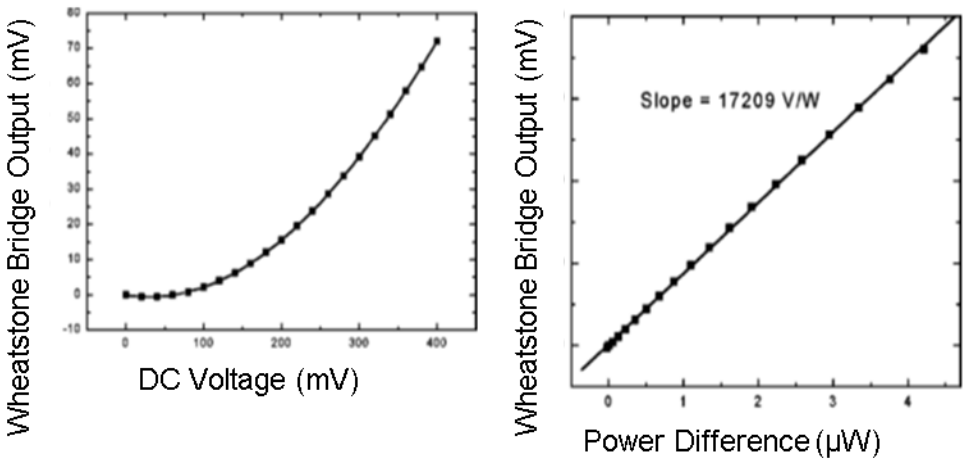

Fig. 3.4 Wheatstone Bridge output dependence on the bias DC offset (left), and the linear dependence of bridge output on the dissipated power [17]

3.1.5 Cell for Bolometer Thermal Capacitance Measurement

The determination of structure thermal capacitance is necessary for determination of time constant. The measurement thermal capacitance is quite similar to the measurement of thermal conductance as mentioned above. The detail of cell for thermal capacitance measurement is shown in Fig. 3.5. There are different sizes of bolometer membranes from (30×30) μm to (50×50) μm in order to determine the thermal capacitance more precisely.

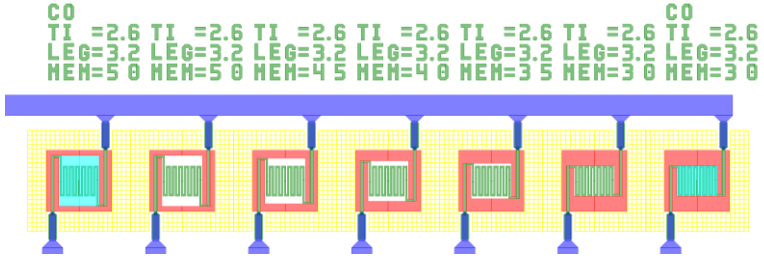

Fig. 3.5 Detail of cell for bolometer thermal capacitance measurement

The equation for V_{OUT} is used to state the relation between the slope S and the thermal capacitance H. Derivation of V_{OUT} equation gives:

$$S = \frac{d\Delta V_{OUT}}{dt} = \frac{\alpha V_B^3}{16 R_0 H}, \tag{3.5}$$

where t is time, α is thermal coefficient of resistivity, and R_0 is the resistance of bolometer at ambient temperature. The Wheatstone bridge is biased by pulse with shorter duration than is an anticipated thermal time constant so the single bolometer chip cools down. The voltage pulse has

a variable peak. Employing this measurement setup, the thermal capacitance can be evaluated [15,21].

3.1.6 Cell for Measurement of Incident IR radiation

This type of cell is designed for IR radiation measurement. The cell consists of the single bolometer chips with the exactly same size namely titanium electrode width is 2.6 μm, the leg width is of 3.2 μm, and the membrane with size of 40×40 μm square. The cell is meant for reference measurement using Wheatstone bridge circuit as described in the read-out circuit chapter.

The bolometer intended for measurement of IR radiation is with Co layer, and the reference one is with reflection Al layer as shown in Fig. 3.1. Comprehensibly, both types of bolometers have to be of the same dimension parameters.

3.1.7 Series-Parallel Bolometer Combination Cell

The measurement using series-parallel cell compares the sensitivity of each combination. Consider the parallel combination for instance is part of Wheatstone bridge instead of single bolometer cell. The measurement employs desired bolometer combination with CNTs (Co layer in the design), and the reference combination with a reflective aluminium layer.

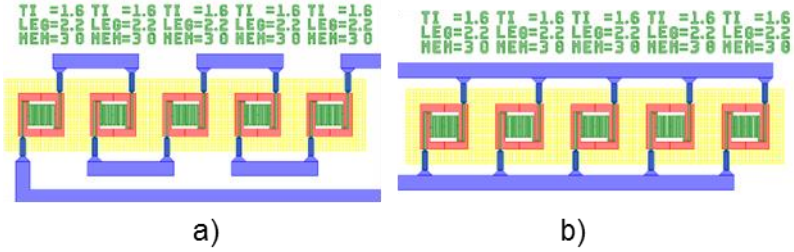

Fig. 3.6 Detail of series-parallel bolometer combination cell

4 Thermal Mechanical Simulation and Analysis

The thermal mechanical simulations are necessary for the optimizing of design and following fabrication of the bolometer chip. These types of simulation help to improve the design and to estimate the mechanical behavior of the structure. Considering the absorption layer is nanostructured, the mechanical performance of bolometer has to be predicted as precise as possible. There is need to evaluate the mechanical stress during the high temperature fabrication as well as during the bolometer operational mode so the designed structure is suitable for this type of device. If any of this critical parameter seems to be out limit there is a chance to redesign the chip or change the fabrication process technologies.

The other important parameters are the self-heating, IV curve, time constant of bolometer, and value of the ambient temperature resistance. The CoventorWare software has been used to thermal mechanical simulation in this work. It is an integrated tool for designing and simulating the MEMS devices. It combines the complete design and the real setup of fabrication process.

4.1 Material Properties Used in Simulation

The material properties data has to be selected carefully because the material properties significantly affect the simulation results. Materials properties are dependent on the fabrication process employed to realize the defined material layer. Detailed complete fabrication process is described in the separate chapter. In the **Table 1** the materials properties are listed exactly in the form the simulation processor works with them.

The stress included in the table defines the stress introduced during the fabrication process. For example, this value is very important to define the von Mises stress of PECVD oxide layer during the bolometer operation. This parameter also helps to explore stress issues between numbers of layers.

The source of the material database is mainly the database of the MIT (Massachusetts Institute of Technology) [29]. This database contains the specific data including the fabrication process. It is well known bulk properties are in some case completely different from the thin films properties. For instance, the silicon dioxide SiO_2 is to be deposited by plasma enhanced chemical vapor deposition (PECVD) which significantly reduces the value of mechanical stress which is significant difference compare to SiO_2 deposited by thermal oxide with high stress. The tensile or fracture stress listed in table shows the limit of roughness of the structure. In case, the simulation results shows during any state of bolometer higher value than fracture stress, the design has to be changed including the thickness of affected layer.

Table 1 Material properties involved in the simulations

Property of Material	Silicon(100)	PECVD SiO_2	Aluminum	Titanium	Cobalt
Young's modulus [MPa]	1.30E+05	8.50E+04	7.70E+04	1.03E+05	2.12E+05
Poisson ratio [-]	0.278	0.25	0.3	0.33	0.32
Density [kg/μm^3]	2.33E-15	2.20E-15	2.30E-05	4.05E-15	8.80E-15
Stress [MPa]		2.50E+02	130	4.39E+02	
Tensile or fracture strength [GPa]		9.52E+00	0.07	2.35E-01	
TCE Integral Form [1/K]	2.49E-06	5.60E-07	2.31E-05	9.50E-06	1.25E-05
Thermal conductivity [pW/μmK]	1.57E+08	1.10E+06	2.40E+08	2.19E+07	6.29E+07
Specific heat [pJ/kgK]	7.03E+14	1.00E+15	9.03E+14	5.28E+14	4.40E+14
Electrical conductivity [pS/um]	1.40E+09	7.00E-07	3.54E+12	2.56E+12	1.60E+12
Dielectric constant [-]	11.8	5.00E+00			

4.2 Setting of Fabrication Process

The fabrication process in CoventorWare is defined to create 3-D model. Initially, the 2D layout created. In this case, the 2D layout is imported bolometer design shown in the chapter 3. The CoventorWare fabrication process defines the 3D structure. There is also a possibility to export this fabrication process file and use to real fabrication of the bolometer chip. The fabrication process in simulation defines the physical relationship between the layers. The complete fabrication setting for simulation is shown in Fig. 4.1.

The setting of fabrication process is corresponding with the actual fabrication process. The thickness of each layer or structure is listed in micrometers. Mask name is connected to the design name according of the 2D layout. Techniques of deposition (sputtering, evaporation)

create the layer model and the following etching process is to pattern the structures designed in 2D layout defined by the etching thickness or certain layer which should be completely removed.

Number	Step Name	Layer Name	Material Name	Thickness	Mask Name	Photoresist	Depth	Mask Offset	Sidewall Angle
0	Substrate	Substrate	SILICON_100	50	SubstrateMask				
1	LPCVD	PECVDSIO2_bottom	PECVD_sillicon_dioxide_Vojta	0.3					
2	Sputtering	Al_pads	ALUMINUM(FILM)	1					
3	Generic Wet Etch				Al_pads	+		0	0
4	Sputtering	Ti_electrode	Titanium_PVD_film	0.03					
5	Generic Wet Etch				Ti_electrode	+		0	0
6	LPCVD	PECVDSIO2_upper	PECVD_sillicon_dioxide_Vojta	0.3					
7	Evaporation	Co_layer	Co_film_bulk_properties	0.05					
8	Generic Wet Etch				Co_IR_layer	+		0	0
9	Sputtering	Al_layer	ALUMINUM(FILM)	0.1					
10	Generic Wet Etch				Al_IR_layer	+		0	0
11	Generic Dry Etch				PECVDupper	-		0	0
12	Generic Dry Etch				PECVDbottom	-		0	0
13	Generic Dry Etch				Silicon_substrate	-	40	0	0

Fig. 4.1 User interface of setting the fabrication process

4.3 Creating 3-D Model and Mesh Settings

The 3-D model (shown in Fig. 4.2) is created using the data of fabrication process and the design. In the figure a single bolometer cell is shown. CoventorWare analyzer solvers are able to approach to the numerical solution of partial differential equations with many different methods depended on the simulation type.

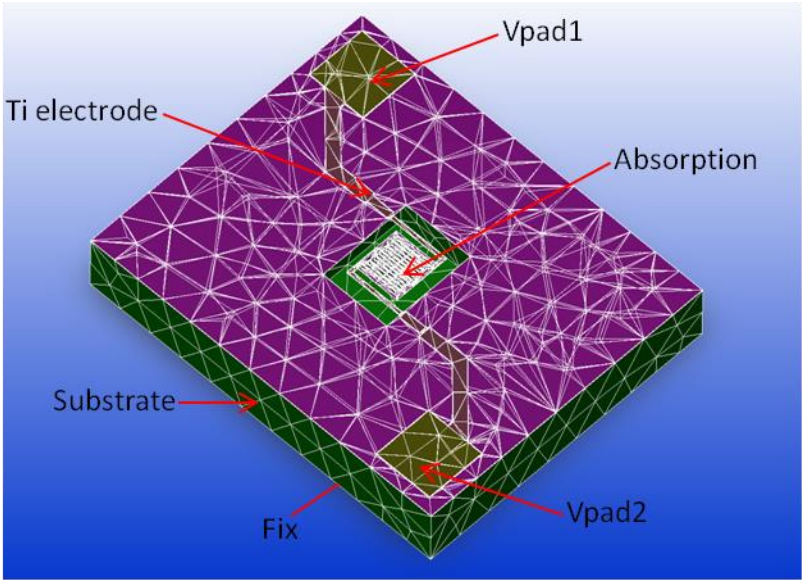

Fig. 4.2 The 3-D model of bolometer single chip structure

The 3-D model serves, of course, for the setting of the simulation. During the setting of 3-D model is necessary to choose which material is conductive and which material is dielectric in terms of simulation. The aluminum for the pads and titanium for electrode are the only materials set to be conductive. The rest of materials (SiO_2, Si, Co) are set as dielectric for purpose of the

simulation. The setting of each contact path is following. The single contact path of this structure and pads for applying voltage are defined using face selection and the setting name of each face. Vpad1 and Vpad2 are face name for applying voltage on the titanium electrode, face fix of the substrate bottom is for mechanical fixing. The substrate in the figure is not included for calculation of the mechanical stress or displacement, not even for the temperature distribution, but it mainly is to mechanically fix the model, and to provide the heat sink. Absorption is name of face for simulating the incident IR flux on the structure.

The cross view can be seen in Fig. 4.3. It is obvious the structure of bolometer membrane is in the space suspended by the oxide beams with embedded Ti electrode. Consecutively, it is obvious to determine the tension of beams to avoid the beam fracture especially during high temperature operation.

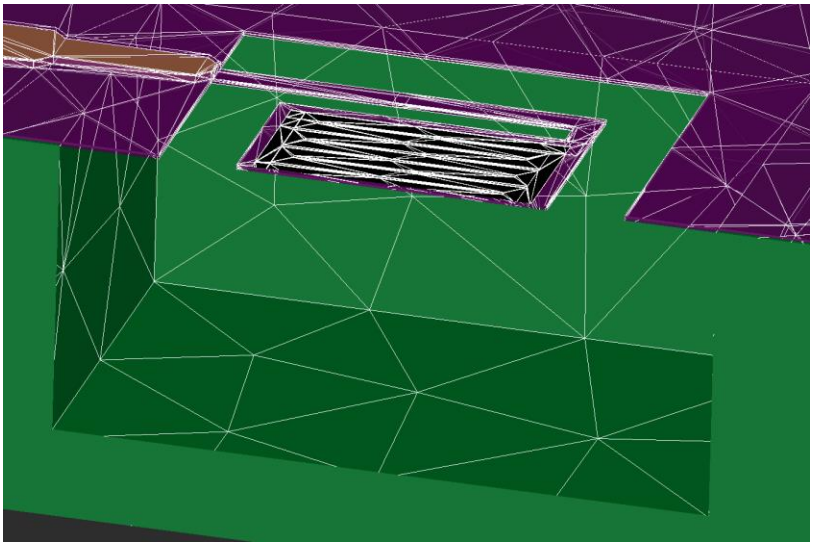

Fig. 4.3 Cross view of bolometer suspended membrane

The mesh type is “hezahearda” type strongly recommended for the thermal-mechanical solution. Element order is parabolic and the element size is 30. The element size is much smaller on the beams of suspended membrane because there is expected to be higher mechanical tension, thermal gradient and possible difficulties with the complete breakdown of whole structure.

4.4 Simulations and Results

This part of thermal mechanical simulation chapter includes the solver simulation setting for each simulation and discuss the simulation results represented by 3-D results or table of values.

4.4.1 Solver Settings for Thermal Distribution and Displacement Analyze

The main solver of CoventorWare is set to "ElectroThermalMechanical" due to studying the structure during applying the voltage and determining the thermal, and consecutively, the mechanical behavior of suspended membrane. This procedure has been used to optimize the final design for bolometer device.

The simulation setting contains the bias voltage applied on the Vpad1 with value of 0.8 V and Vpad2 of 0.0 V in order to determine the steady time dependence of temperature. The face named fix is set to be fixed in all directions to represents the reference for the displacement analyze. The initial temperature is set to 300 K but it is not necessary if the simulation is not transient. The substrate is with the fixed temperature of 300 K to secure the heat sink.

4.4.2 Results of Thermal Distribution and Displacement Analyze

The first result is the temperature distribution for final design bolometer structure shown in the Fig. 4.4. The simulation is performed for steady state according to the CNT's fabrication. During the CNT's growing, it is requested to locally heat the suspended membrane. Not surprisingly, the temperature is heating the membrane most which is an ideal distribution for CNT's growing. Another important fact is the power consumption of bolometer will be not so high which is in correspondence in nowadays' energy trends. The bending of the membrane is also obvious. Displacement maximum of the structure is 6.4 μm. This value seems not be critical for conventional MEMS application but it could cause some unexpected issues for the nanostructured surfaces employing in this thesis.

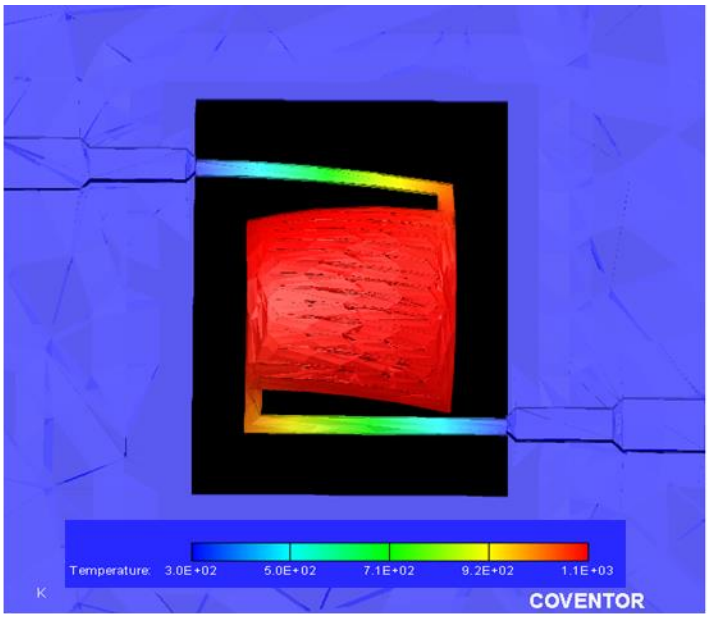

Fig. 4.4 The thermal distribution of bolometer membrane

In order to reduce the bending of the suspended membrane, there is comparing of different designs using different types of beams, membrane sizes, and the alternative structure modification which is reported below.

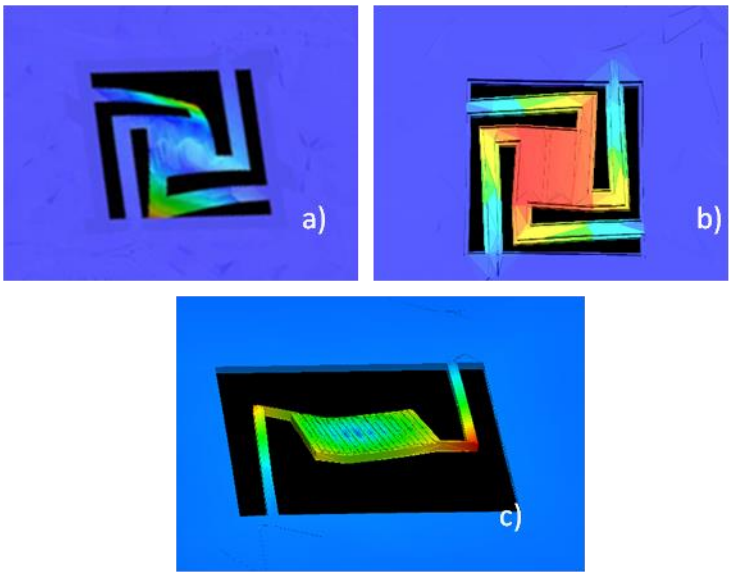

Fig. 4.5 Displacement of different membrane design

The simulation results for different designs are shown Fig. 4.5. For every design, the simulation setting is the same listed above. In the Fig. 4.5 a) is shown the typical design for suspended membrane and it is clear the bending is significant. Furthermore, there are four beams which increase the value of thermal conductance of the membrane and proportionally increase the power consumption.

The new technique is represented by the Fig. 4.5 b). It can be seen the structure is not bending rather than rotating itself. The value of displacement in Z axe is in the order of 100 nm. Corresponding to that result, there is no problem for the intended nanostructured surface of the membrane.

The design (shown in Fig. 4.5 b)) is done employing so called trenches which have been already reported [21]. In this thesis these trenches are modified for the purpose of suspended membrane. The fabrication of trenches is as follows. The silicon substrate is without oxide etched using DRIE (deep dry ion etching) to create a shape for the trenches. The CVD SiO_2 is following and as the SiO_2 is deposited is the etched pattern the trenched are built. The polishing of the SiO_2 is recommended to gain the oxide layer with the homogenous thickness. In the presented design, the trenches are applied under beams and under square perimeter of the membrane plate.

The last optimizing (shown in the Fig. 4.5 c)) is done with designing just two beams. Applying this design, the thermal conductance is not critical for power consumption or bolometer

response characteristics. There is turning as whole plate so it is not critical for nanostructured surface. The final design is choose to be similar to this one and is described in the chapter 3.

4.4.3 Solver Setting for Steady Time Analyses

In this part, the simulation is determining the relationship between the applied voltage and the temperature, and the current varies with voltage dependence. The values of mechanical stress and tension are to be investigated, as well. The solver is the electrothermal. The voltage applied on Vpad1 is set to be parametric in interval 0.0–0.8 V. The step for parametric study is 0.01 V. The Vpad2 is with voltage of 0.0 V. As in previous simulations the substrate temperature is 300 K.

4.4.4 Results for Steady Time Analyses

Fig. 4.6 shows the temperature dependence on the applied voltage. This parameter is relevant for the operation, but also, the fabrication process of bolometer namely the CNT's deposition. In case of CNT's deposition the temperature of membrane has to be 600 °C. According to the simulation results the applied voltage should be 0.44 V. The temperature increment is caused mainly due to self-heating effect. When the measurement of bolometer properties is proceeded the voltage pulse is with value of 2.5 V. In the case of applying 2.5 V on the bolometer structure it is obvious that the structure would be damaged.

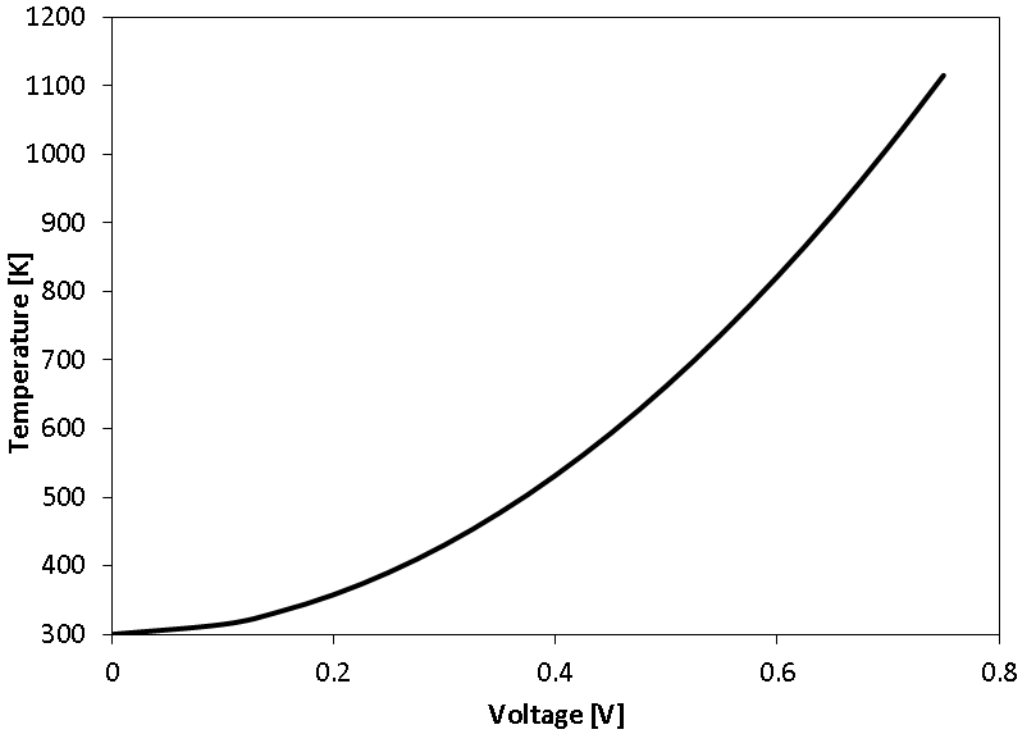

Fig. 4.6 Temperature dependence on applied voltage

The IV curve is shown in Fig. 4.7 and represents the current varies with the voltage. The dependence is linear which is necessary for the IR detection measurement. The linear dependence is mainly caused by using the Ti electrode for bolometer. Another advantage, the titanium is also stable in the bolometer operation temperature range.

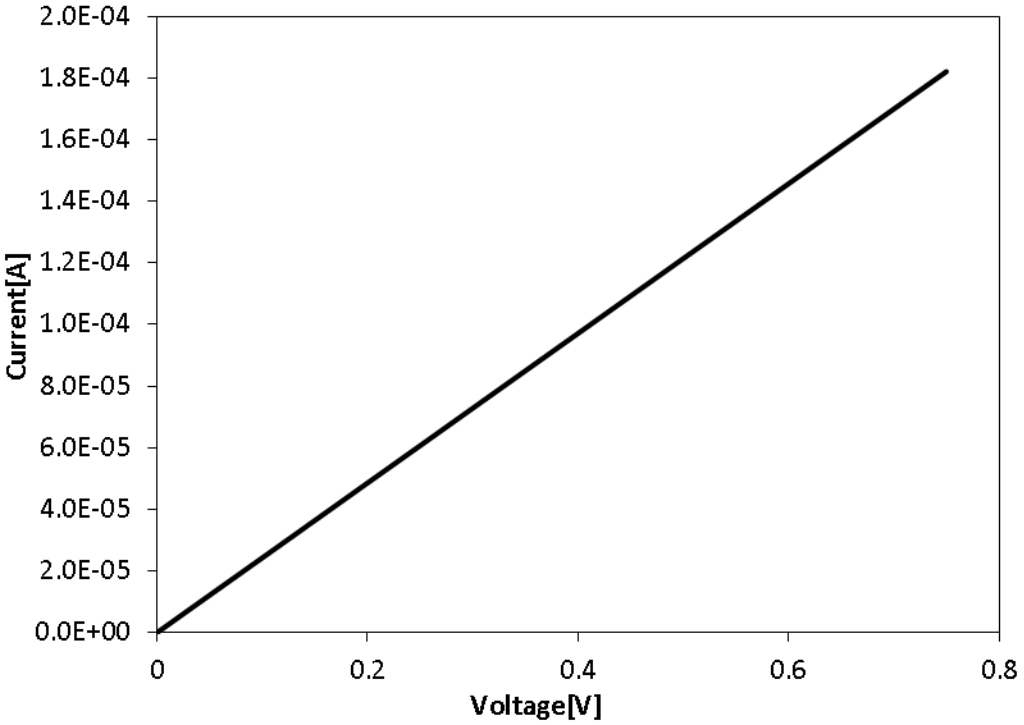

Fig. 4.7 I-C curve of bolometer chip

The maximum value of the mechanical stress is very critical for design and for the fabrication process plan including chosen materials. In the Fig. 4.8 is shown the von Mises stress relationship with the temperature for the bottom layer of SiO_2 in other words, the first deposited oxide. The temperatures for which the simulation is done are much higher than it is limit for the operation state of bolometer. This fact is well presenting the structure behavior during mentioned conditions.

The von Mises stress of upper layer is shown in the Fig. 4.9. The linear dependence is for the upper layer of SiO_2 (second deposition). Both SiO_2 is chosen to be done by PECVD deposition which strongly reduces the stress performance so with the different type of deposition the stress value could be much higher.

The highest temperature of bolometer structure is during CNT's growing procedure. The temperature value is 650 C (923 K). The von Mises stress according to the growing temperature is 545 MPa for bottom layer and 1875 MPa for upper. The stress of the oxide material could be around 2 GPa. The fracture stress is around 9.5 GPa. The SiO_2 and this design is supposed to

cause no problem during the fabrication or the operation of the bolometer. Though it is important to remember the structure tension is significantly high.

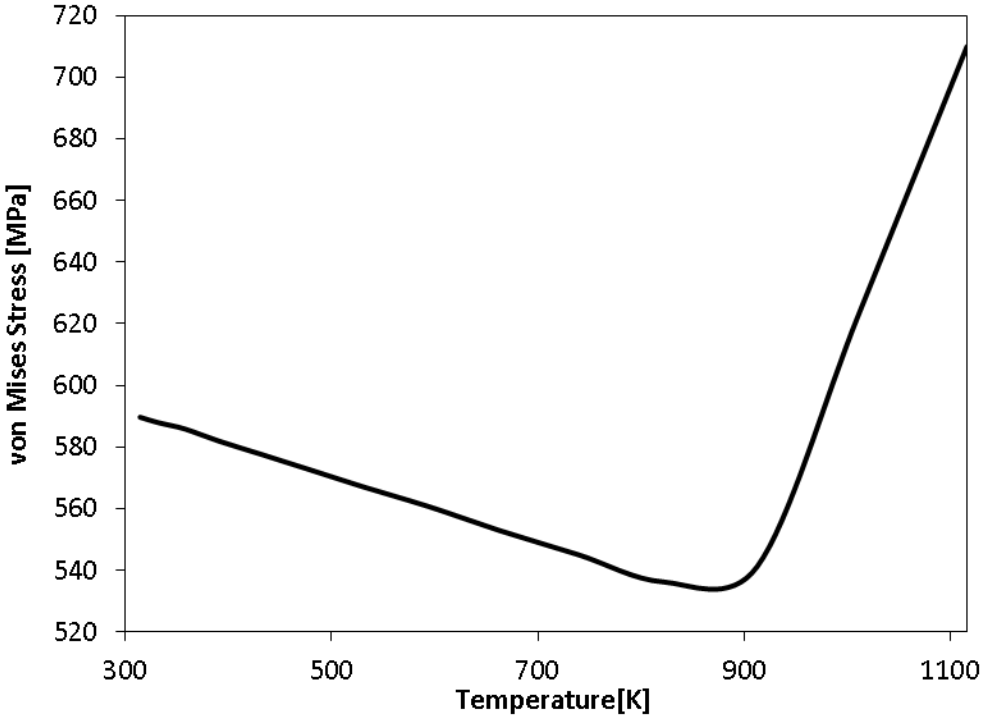

Fig. 4.8 The von Mises Stress of the PECVD SiO_2 bottom layer

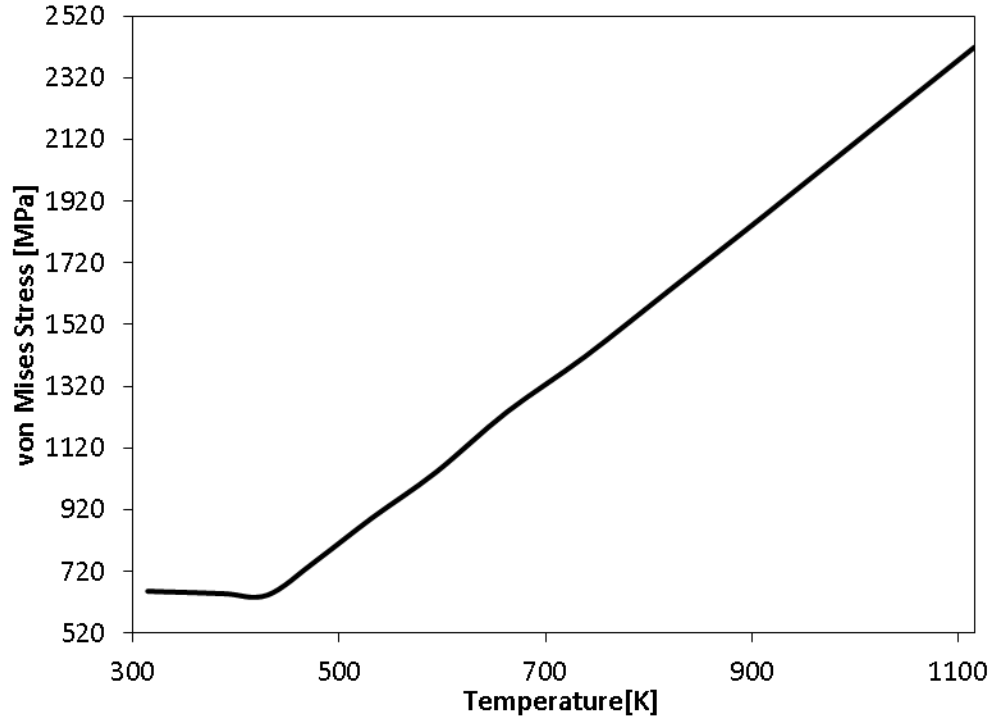

Fig. 4.9 The von Mises Stress of the PECVD SiO_2 upper layer

4.4.5 Solver Setting for Transient Response to Step Voltage

The transient simulation is performed to predict the bolometer response to an input voltage signal. The self-heating effect is studied and the first determination of time constant can be done. The solver of simulation is "ElectroThermal". The applied voltage pulse is with amplitude of 2.5 V and it is 400 μs long. This voltage pulse is applied on the Vpad1 and Vpad2 voltage is 0.0 V. Temperature of the face fix is 300 K. The initial temperature of every bolometer cell part is 300 K. The simulation time is 0.0–0.01 s.

4.4.6 Results for Transient Response to Step Voltage Simulation

The results of transient analyze is plotted in Fig. 4.10. The temperature response to the voltage pulse (2.5 V) is rapid. Considering 2.5 V value of voltage, the temperature is increasing with the rate 1 K/1 μs. The self-heating effect must be considered otherwise the damage of the bolometer is unavoidable. The time response is also limited by the self-heating effect and the time constant of bolometer.

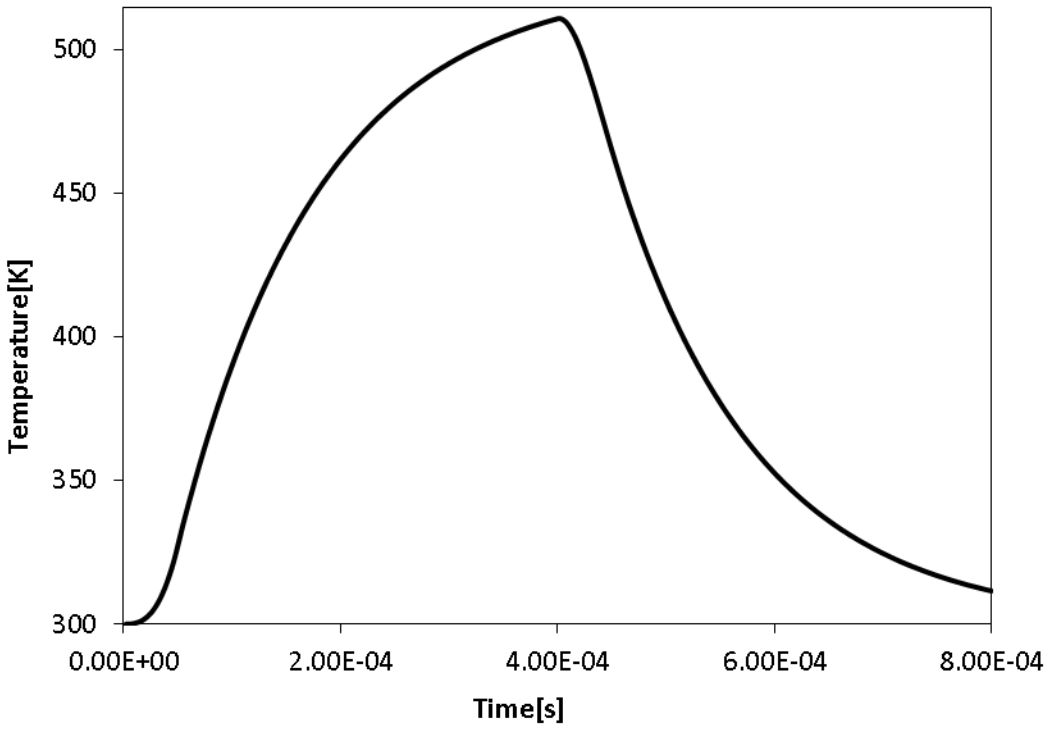

Fig. 4.10 Bolometer temperature response to input step voltage

The illustration of the temperature increase which would be only caused by incident infrared flux is shown in the Fig. 4.11. The signal which has to be removed to detect the incident IR is seen. The temperature change is in the order of 200 K due to self-heating effect and about 0.25 K due to the incident IR flux.

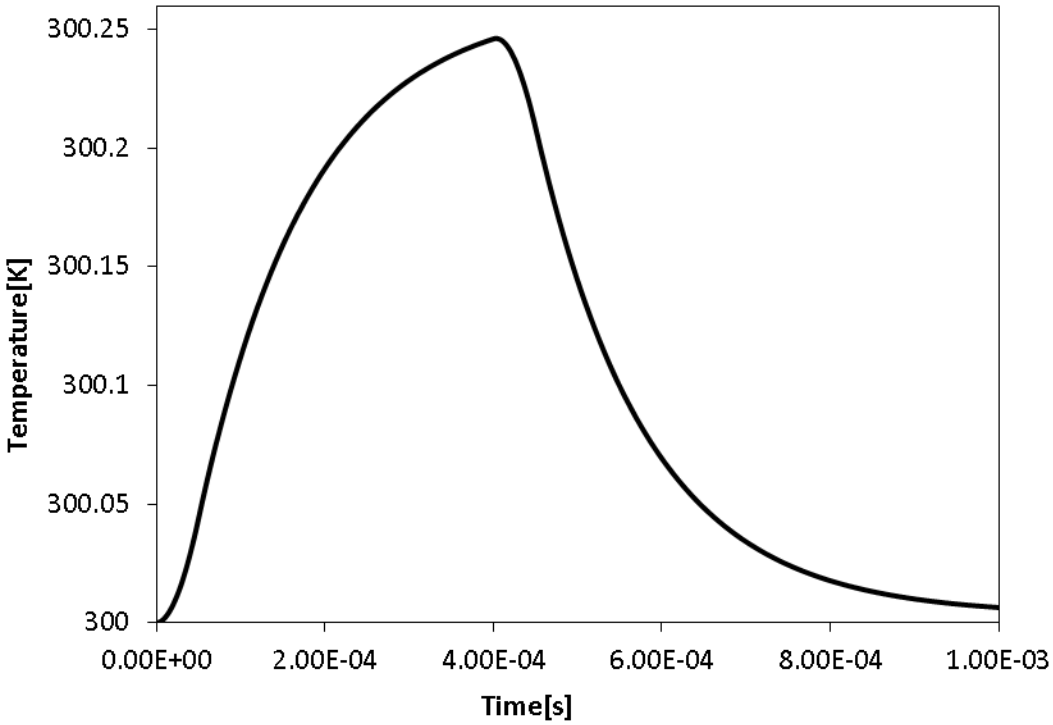

Fig. 4.11 Bolometer temperature response to incident IR flux

4.5 Chapter Conclusion

In this chapter, the process to optimize the design is done. The design shown in the chapter 3 has been done simultaneously with the CoventorWare simulation. The fabrication process has been considered as well. The time response of bolometer is also predicted which is included in the designing of the read-out circuit.

5 PSpice Model of Bolometer Structure

The PSpice bolometer model helps to simulate the read-out circuit for IR detection. Considering purpose of this work, it helps to design and prepare the read-out circuit for bolometer characterization measurements. The values of bolometer thermal properties are measured of the already reported bolometer [17] chip in order to obtain the precise value of bolometer electrical response.

5.1 Electro – Thermal Modeling of IR Bolometer

The bolometer structure contains of an absorption part for IR detection which increases the temperature of chip. Temperature increase is dependent on the thermal capacitance and the thermal conductance. The electrical response is caused by the change in resistivity due to temperature change. Unfortunately, the temperature is changing not just with incident IR but due to self-heating effect as well. These parameters of properties influence the bolometer response behavior. Thermal response of bolometer is appearing in the vacuum so the convection losses to ambient space are negligible. Consequently, the parallel combination of thermal capacitance H and the thermal resistance Z can be used to model the bolometer operation behavior. The thermal resistance consists of two parts: radiation loss to ambient Z_R and the heat conductance of suspended membrane to substrate Z_C. The self-heating power is a function of the input current and the electrical resistance of bolometer. Therefore, the heat balance equation representing the bolometer response can describe as follows:

$$H\frac{d}{dt}T(t) = P(t) - \frac{1}{Z}[T(t) - T_S], \tag{5.1}$$

where the T_S is the temperature of bolometer, $T(t)$ is temperature dissipated across the bolometer structure due to the self-heating effect and the incident IR. The thermal response of the bolometer can be simulated employing the RC circuit. The thermal electrical analogy listed in Table 2 is then employed [15].

Table 2 Thermal electrical analogy list with units

Thermal parameters	Electrical equivalents
Z [K/W]	R_T [V/A]
Z_c [K/W]	R_C [V/A]
Z_R [K/W]	R_R [V/A]
H [J/K]	C [As/V]
T(t) [K]	V(t) [V]
P(t) [K]	I(t) [A]

The heat balance equation can be described using the electrical equivalents and is given as follows:

$$C_T \frac{d}{dt} V(t) = I(t) - \frac{1}{R_T}[V(t) - V_0], \tag{5.2}$$

where V_0 is the reference potential and refers to substrate temperature, C_T corresponds to the heat capacitance, R_T refers to thermal resistance. The voltage $V(t)$ equals temperature caused by self-heating effect and the incident IR. The circuit corresponding with bolometer thermal parameters is in the Fig. 5.1 RC circuit representing the thermal parameters of bolometer.

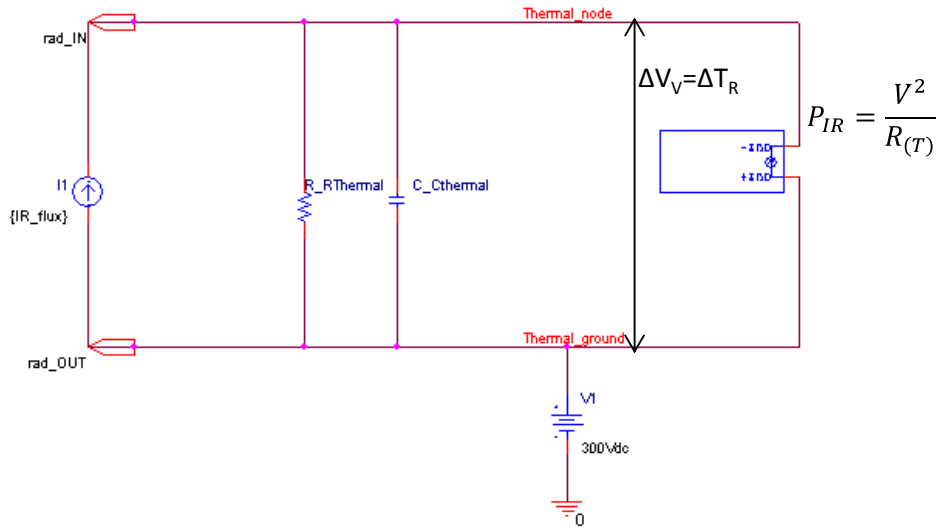

Fig. 5.1 RC circuit representing the thermal parameters of bolometer

The P_R is power due to self-heating with respect to temperature resistance of bolometer. The voltage source represents the substrate temperature. The voltage difference is, obviously, presenting the temperature change. The pins named rad_IN and rad_OUT is for applying the incident radiation. In the terms of electro thermal analogy the source for IR is the current source. The RC cell represents the thermal parameters of bolometer. The implementation of the RC cell is following. The complete bolometer model is presented is the Fig. 5.2.

There has to be careful and special consideration not to confuse the electro thermal analogy and the actual electrical quantities which are presenting bolometer as temperature dependent resistor. On the one side, there is RC circuit representing the thermal properties of bolometer described above. On the other side, there is simple ABM (Analog Behavior Model) which is representing the temperature dependent resistor. The change of resistance is demonstrated as the current change.

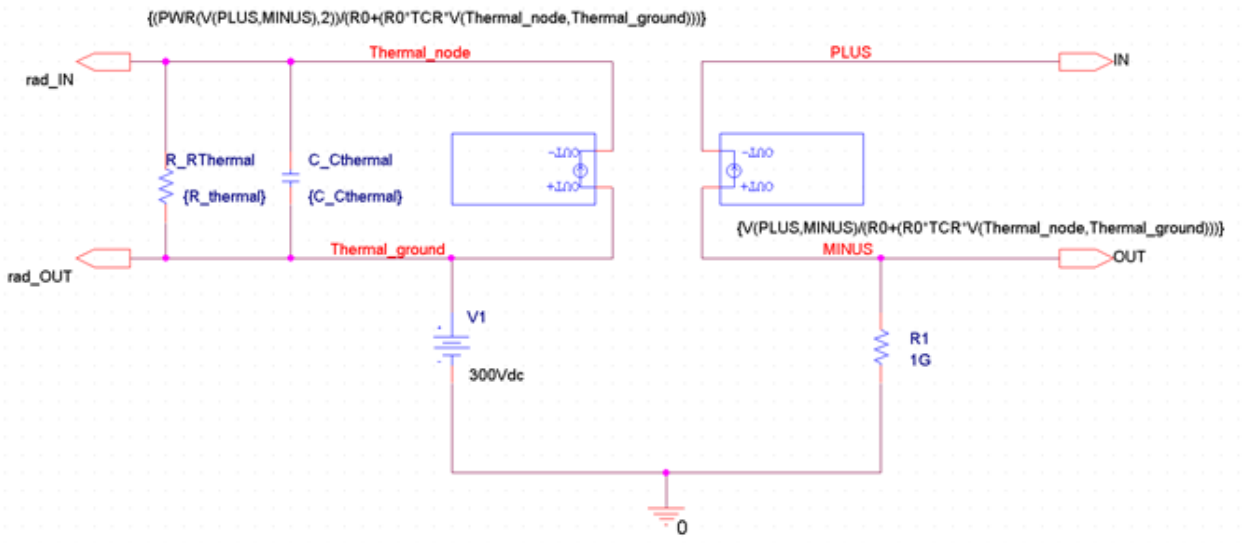

Fig. 5.2 The electrical bolometer model for PSpice simulations

The function for the current change is as follows:

$$i(t) = \frac{V(Plus,Minus)}{R(T)}, \tag{5.3}$$

where i(t) is current flowing through bolometer chip, V(Plus, Minus) is voltage applied on the bolometer pins, and R(T) is resistor changing due to temperature as:

$$R(T) = R\_0\,[1 + TCR{\cdot}V(Thermal\_Node, Thermal\_Ground)], \tag{5.4}$$

where the TCR is titanium thermal coefficient of resistance, the V(Thermal_Node, Thermal_Ground) is referring to the temperature change. The resistance R_0 is the ambient temperature resistance of bolometer. The resistor R1 is for the purpose of simulation solver software.

5.2 Settings for Voltage Response Simulation

The simulation of electrical response has been done using the Cadence OrCAD Caputure software. The Wheatstone bridge is used as the read-out circuit. According to the theoretical part of this work it is obvious the instrument amplifier is necessary to gain decent out voltage. Nevertheless, the response simulation has been done without any amplifier to obtain the bolometer response value. The circuit used in simulation is represented in the Fig. 5.3. The bolometer 2 and the bolometer 3 are presenting the bolometer with the aluminium reflection layer. In other words, these bolometers are used as the reference bolometers. Bolometer 1 and bolometer are the IR detecting bolometers. Current sources are representing the IR flux with the power value of the infra-red radiation.

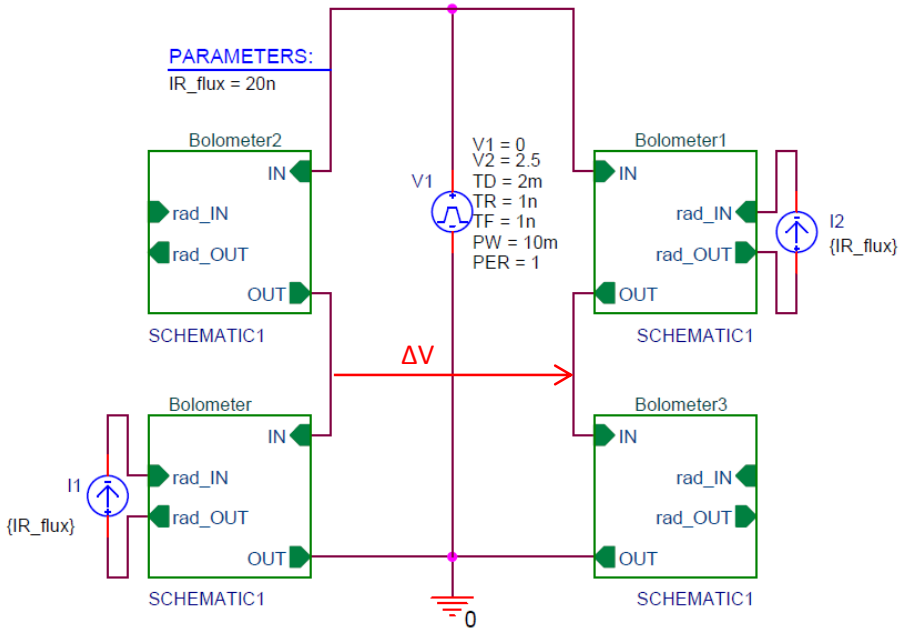

Fig. 5.3 The scheme of simulated bolometer read-out circuit

The voltage pulse for IR measurement is applied by the voltage source V1. The voltage amplitude (V2) is 2.5 V with the pulse width (PW) 10 ms. The period of the measurements has value 1 s. The period is not important for the purpose of simulations but in measuring of fabricated bolometers chips the cooling down of bolometers has to be considered. Using an actual voltage pulse generated the burst mode has to be chosen to obtain this period value. Time delay (TD) is setup to be 2 ms in order to simulation results would clearly approach to the correct voltage response value.

The transient analyze is performed to simulate the voltage response. The calculation time is set up from 0 s to 150 ms. The calculation time step is 100 ns. The performance analyze is then performed to achieve a parametric study for IR lux power value in time of 4 ms. The IR flux power value is from 10 nW to 100 nW represented by the currents sources with value 10–100 nA respecting the thermal electric analogy mentioned above.

5.3 Simulation Results and Conclusion

The simulation results show the time dependence of the input and the output voltage in the read-out circuit. The Fig. 5.4 shows the input voltage pulse and the resulting output voltage of single bolometer chip. The output voltage function is caused mainly due to the self-heating effect of bolometer structure. The IR detection measurements are mostly done in the time of 4 ms.

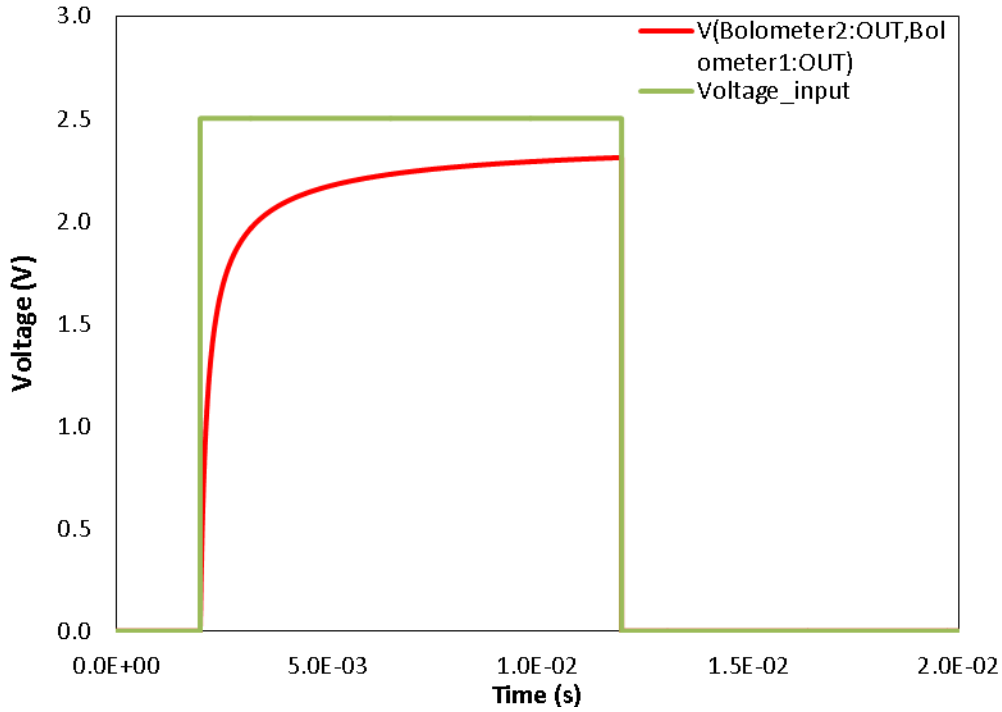

Fig. 5.4 Time dependence of the input voltage pulse and the output bolometer voltage

The performance analyze results are shown in the Fig. 5.5. There is a plot of differential voltage dependence on the incident IR flux power. The function representing this dependence can be described as linear function. It is obvious that the change of differential voltage is in the range of 100 nV. The values of voltage are very low and the output signal has to be amplified otherwise the noise issue could appear.

In order to increase the sensitivity of bolometers the serial parallel combinations have been investigated. In the chapter 3 the design serial parallel type cells is shown and described. The transient analyze for these combination including the parametric study of IR flux power has been done. The results are listed in the Table 3. The value for single bolometer differential voltage is approximately 100 nV as mentioned above. The parallel combination works as the summary of the bolometers. However, the serial combination has the differential voltage with value of 3.2 μV using the same simulation parameters and conditions as with previous combination. It seems the serial combination improves the sensitivity of device. The best sensitivity results show the combination of serial and parallel bolometer array contained of 4 bolometers.

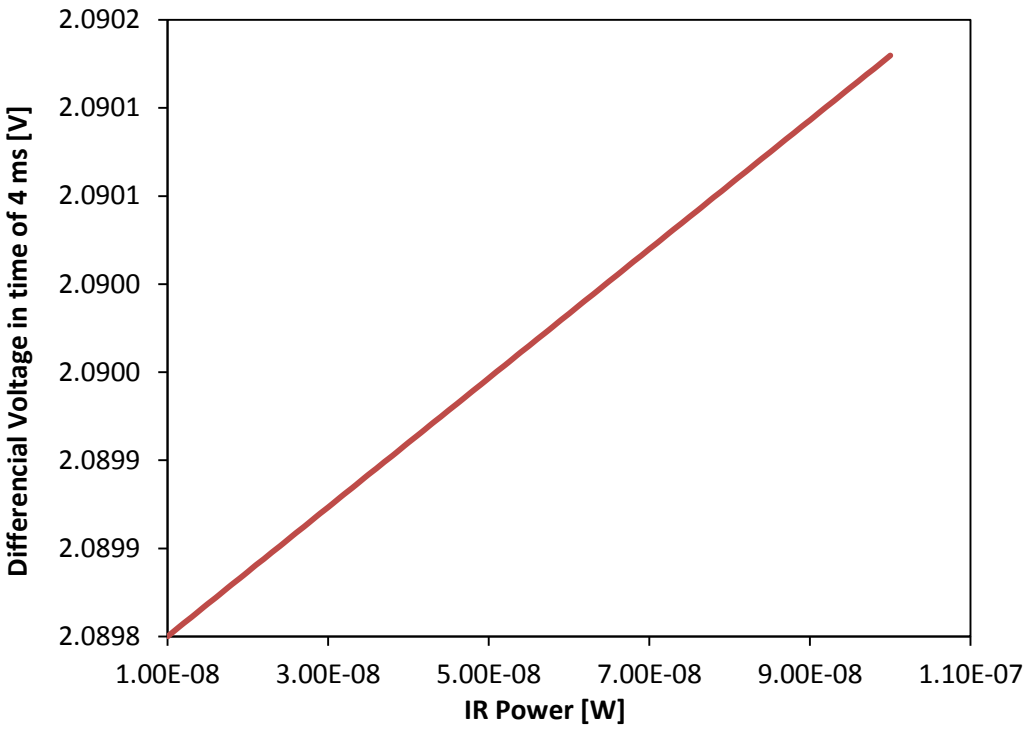

Fig. 5.5 Differential voltage dependence of the initial IR flux value

Table 3 The differential voltage value for serial parallel combination of bolometers

Simulation comparison of serial/parallel combination			
Combination	$V1_{40}$[V]	$V2_{70}$[V]	ΔV [V]
Single Bolometer	2.09	2.0901	0.0001
Parallel Combination	2.0905	2.0911	0.0006
Serial Combination	1.4634	1.4666	0.0032
Serial Combination	0.8108	0.8148	0.004
Serial-Parallel 2x2	1.5478	1.5524	0.0046

5.4 Chapter Conclusion

The PSpice model of bolometer is designed to simulation the bolometer voltage response. It is important to know the approximate value of differential voltage to adapt the measurement circuit for this device. The simulation results show the differential voltage order of 100 nV. For the measure purpose the instrument amplifier AD8221 by Analog Devices will be used to avoid problems with the noise and to optimize the detection of the device. Study of the bolometer combination shows the serial combination of bolometer also helps to obtain better response. This result is quite expected since the read-out circuit is working with the constant voltage value and the current flowing through the bolometer electrode is changing.

6 Fabrication of Bolometer Chip

The fabrication of bolometer is mostly the contained of elementary silicon technology processes. In this part of the work, the fabrication plan including elementary steps details is described. The CNTs layer deposition on chip is presented. This technological process has been never tested or performed before this project.

6.1 Fabrication Process Plan Overview

The fabrication process plan is using the design described in the chapter 3 and selected materials which are overviewed in the chapter 4. The Fig. 6.1 represents the fabrication process not including lithography.

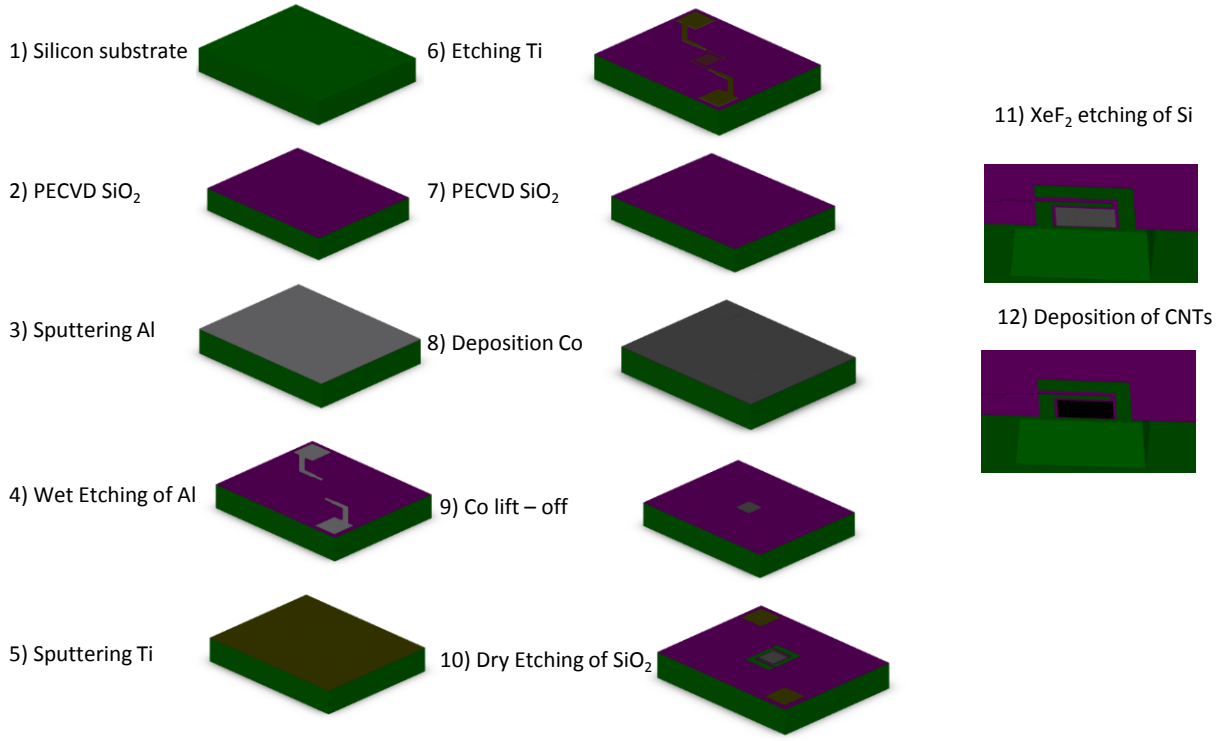

Fig. 6.1 Schematic representation of bolometer fabrication process

The fabrication process starts with silicon substrate (100). The plasma enhanced chemical vapor deposition PECVD of SiO_2 with thickness 300 nm is following. The magnetron sputtering is then use to deposit the aluminium layer with thickness of 1 μm. The lithography employing the lithography mask for pattering Al (shown in Fig. 3.1) is then use to pattern the resist as the protective layer for Al etching. The Al etching is done by H_3PO_4 based etchant to avoid damaging the underlying oxide layer. The process continues with the resist striping. Titanium

deposition with thickness of 30 nm using the magnetron sputtering is then proceeded. The Ti sputtering has to be done with minimal value of the impurities of layer in order to create the temperature sensing electrode. The lithography employing the mask for pattering Ti is done to create the protective layer for Ti etching. The etching of Ti by NH_4OH/H_2O_2 based etchant to avoid damaging of the SiO_2. When the Ti electrode is pattered, the stripping of the resist is happening. The deposition with the same parameters as the first PECVD SiO_2 with thickness of 300 nm is consecutively done. On the deposited oxide layer, the aluminium film is created by magnetron sputtering with thickness of 100 nm. The lithography for pattering of the layer is then performed using the mask for pattering the second aluminium layer. During the process, the same type of etchant as the first Al etching is used. After stripping the resist, the lithography is for cobalt layer is following. The Co film deposition using the thermal evaporation is then proceeded with the thickness of 5 nm. The lift-off procedure to pattern the Co layer is consecutively done. The lithography with mask for SiO_2 etching is then performed. The etching is done by CHF_3 plasma stopping of the silicon or Al bonding pads with the resist as the protective layer. The releasing of the membrane is following. The etching is performed by XeF_2 which does not etch the SiO_2, Al, and Co. When the membrane is obtained, the CNT's deposition on chip can be performed.

6.1.1 CNTs Deposition on the Chip

The CNTs deposition on the chip is new technique especially designed for fabrication of bolometer chip. The CNT deposition is last and one of the most critical fabrication steps of process. Consider the fabricated bolometer structure after XeF_2 etching when the membrane is released. The bolometer chip connected to the special designed package using wire bonding. The Fig. 6.2 represents the idea of the deposition process procedure with already connected bolometer chip. According to the thermal mechanical simulations the temperature is dissipated on the membrane so the Al pads and other thermal sensitive parts are not damaged. The growing of the CNTs are appearing only on the membranes with Co layer.

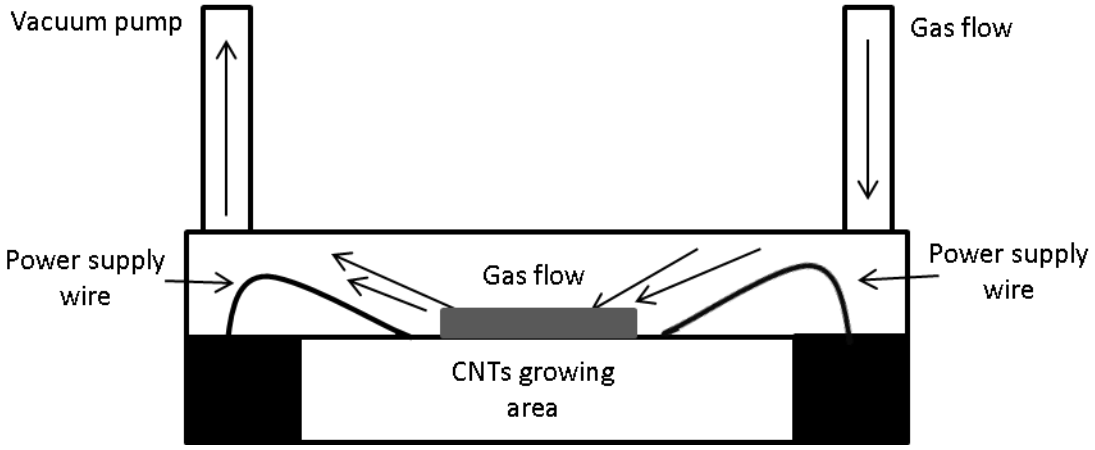

Fig. 6.2 The scheme of CNTs deposition on the chip process

The gas is flowing controlled by the gas flow controller with the value close to the value mentioned in the FT-IR chapter. Voltage is set up to obtain the temperature for CNTs growing. The values have to be experimentally achieved.

6.2 Fabrication Process Conclusion

The fabrication of bolometer is one of the main tasks of this thesis. However it has appeared to find the clean room with all necessary equipment. The complete fabrication process represents nothing challenging for the standard microtechnology. With the only exception presented during the CNTs deposition on the chip which has to be experimentally optimized. The experimental chips fabrication process has been started. There were some critical problems during the first etching of the aluminium layer. Many experiments have been done to choose the right type of developer which would not under etch the resist pattern. The following steps were done without significant difficulties. The DRIE etching of the SiO_2 is the step which, unfortunately, has been the last unfinished fabrication process. Also, the fabrication has not been done in the one laboratory which results in the decreasing quality of the fabricated devices. Therefore, there has to find new facility to fabricate the bolometer chips.

7 Conclusion

This thesis task is to investigate the microbolometer using carbon nanotubes for infrared detection. The microbolometer is supposed to be fabricated using MEMS technology. The applying of carbon nanotubes as the absorption layer is the new approach for IR detection technology.

In theoretical part, there is the bolometer operation principle description to show the possibilities of bolometer design, fabrication and how to achieve the improvement considering the recent application of infrared detection field. There is an overview of nowadays IR technology and short mention of history as well. The important part is the principle description of bolometer operation. Many aspects to bolometer operation are mentioned and the read-out circuit is studied. There are mathematical relations of bolometer physics, its operation, and the output signals overview. The physical parameters are then used in the following parts of the thesis. The commonly used design is then represented and the field array of bolometer is mentioned even if the task of this work is not to create the bolometer array field.

The CNTs theoretical study is not involved particularly in this thesis. Nevertheless, there is some fundamental description in the part of the absorption layer characterization. The measurement to verify the CNTs are improving the IR absorption is done by FT-IR method. The CNTs deposition conditions are presented. The Co layer is applied as the catalytic layer for CNTs growth which is the same layer planned to use in the bolometer fabrication process. The FT-IR measurements show the CNTs layer has absorption with high value about 1.

This thesis contains the final design of bolometer which will be used for bolometer fabrication, characterization measurements, and to verify the improvement of bolometer infrared detection. The design part is the practical part of the thesis; nevertheless, there is theoretical background for bolometer parameters measurement. The design description of different cell types is in the chapter 3 as well. The characterization measurement for major parameters namely thermal conductance, thermal capacitance, and thermal time constant is described and planned. As the final design the suspended membrane is chosen in order to achieve fast response of IR detection measurement. The design part had been optimized employing the thermal mechanical simulation results from the following part of the work.

Thermal mechanical simulations are very important part of this work. The final design had been used to verify that stress values are not critical considering the operation of bolometer. The self-heating effect is studied using the transient analysis. There is a comparison of the temperature change due to self-heating, regarding to temperature change due to power of IR flux. The temperature dependence on voltage is investigated. The determination of bolometer ambient

temperature resistivity is evaluated in this chapter. The new structure design is presented in this part of the work. This design applies so called trenches to the suspended membrane structure. It helps to solve the problem with bending of the membrane which is not allowed for the nanostructured membrane surface.

The PSpice model has been created in the chapter 5. The model is created using the electrical thermal analogy. The purpose of this model is to simulate the voltage response of bolometer. The model combines the thermal and the electrical properties. The read-circuit is then optimized considering these simulations results. The Wheatstone bridge is the simplest read-out circuit and has been simulated to estimate the value of the differential voltage.

The complete fabrication process is then presented is this work. There is an explanation of using the particular technology and the connection with the masks of the design chapter 3. The new approach to CNTs deposition is presented and described. The fabrication process has not been successfully finished. There have been many difficulties and the time delay finally caused the fabricated chips are not presented in this thesis. Therefore, the characterization measurements have not been performed as well. Nevertheless, the fabrication will be finished and the measurement will be following. This thesis contains the final design approach, the complete detailed fabrication plan, and the absorption layer characterization. The bolometer using CNTs as absorption layer is new technology for IR detection. Therefore, the tasks of the thesis have not been fully completed.

8 References

[1] MERRIAM-WEBSTER. Merriam-Webster Dictionary. [online]. 2.12.2013 [cit. 2.12.2013. Available from: <http://www.merriam-webster.com/dictionary/bolometers>.

[2] ROGALSKI, A. Infrared detectors: an overview. *Infrared Physics & Technology*, 2002, vol. 43, no. 3–5, pp. 187-210. ISSN 1350-4495.

[3] TANAKA, A. et al. Infrared focal plane array incorporating silicon IC process compatible bolometer. *Electron Devices, IEEE Transactions on*, 1996, vol. 43, no. 11, pp. 1844-1850. ISSN 0018-9383.

[4] FRANK NIKLAUS, C. V., HENRIK JAKOBSEN MEMS-Based Uncooled Infrared Bolometer Arrays – A Review. *MEMS/MOEMS Technologies and Applications III*, 2007, vol. 6836, pp. 15.

[5] ThesisSTETSON, S. W. *PSpice Modelling and Parametric Study of Microbolometer Thermal Detectors*. Duke University,

[6] SCHAUFELBUHL, A. et al. Uncooled low-cost thermal imager based on micromachined CMOS integrated sensor array. *Microelectromechanical Systems, Journal of*, 2001, vol. 10, no. 4, pp. 503-510. ISSN 1057-7157.

[7] TAE-SIK, K. a HEE CHUL, L. A Highly Sensitive Bolometer Structure With an Electrostatic-Actuated Signal Bridge. *Electron Devices, IEEE Transactions on*, 2006, vol. 53, no. 9, pp. 2392-2400. ISSN 0018-9383.

[8] MASSOUD, M. *Engineering thermofluids : thermodynamics, fluid mechanics, and heat transfer*. Berlin: Springer, 2005. pp. ISBN 3540222928.

[9] HALLIDAY, D. et al. *Fundamentals of physics*. 6th. New York: Wiley, 2001. 1300 pp. ISBN 0471332364

[10] HSU, T.-R. *MEMS and microsystems : design, manufacture, and nanoscale engineering*. 2nd. Hoboken, N.J.: John Wiley, 2008. pp. ISBN 9780470083017.

[11] KIRAN, S. R. a KARUNASIRI, G. Electro-thermal modelling of infrared microemitters using PSPICE. *Sensors and Actuators A: Physical*, 1999, vol. 72, no. 2, pp. 110-114. ISSN 0924-4247.

[12] ThesisDECHARAT, A. K. T. H. G. S. F. R. E.-O. S. *Integration and Packaging Concepts for Infrared Bolometer Arrays*. Stockholm: Skolan för elektro- och systemteknik, Kungliga Tekniska högskolan, 9789174153378 9174153374.

[13] SVATOS, V. et al. Design and Fabrication of MEMS Low Power Heating Membrane. *ElectroScope*, 2012, vol. VI, pp. 1-3. ISSN 1802- 4564.

[14] ANDREA CATALANO, A. C., JEAN-MICHEL LAMARRE An analytical approach to optimize AC biasing of bolometers. *Optical Society of America*, 2010.

[15] GU, X. et al. Determination of thermal parameters of microbolometers using a single electrical measurement. *Applied Physics Letters*, 1998, vol. 72, no. 15, pp. 1881-1883. ISSN 0003-6951.

[16] RAMAKRISHNA, M. V. S. et al. Highly sensitive infrared temperature sensor using self-heating compensated microbolometers. *Sensors and Actuators A: Physical*, 2000, vol. 79, no. 2, pp. 122-127. ISSN 0924-4247.

[17] NEUZIL, P. a MEI, T. Evaluation of thermal parameters of bolometer devices. *Applied Physics Letters*, 2002, vol. 80, no. 10, pp. 1838-1840. ISSN 0003-6951.

[18] SAXENA, R. S. et al. PSPICE circuit simulation of microbolometer infrared detectors with noise sources. *Infrared Physics & Technology*, 2012, vol. 55, no. 6, pp. 527-532. ISSN 1350-4495.

[19] SIRINGO, G. Technical description of LABOCA. [online]. [cit. Available from: <http://www.apex-telescope.org/bolometer/laboca/technical/>.

[20] Conference ProceedingsKIMATA, M. *MEMS-Based Uncooled Infrared Focal Plane Arrays*. Solid-State Sensors, Actuators and Microsystems Conference, 2007. TRANSDUCERS 2007. International. 10-14 June 2007.

[21] NEUZIL, P. et al. Micromachined bolometer with single-crystal silicon diode as temperature sensor. *Electron Device Letters, IEEE*, 2005, vol. 26, no. 5, pp. 320-322. ISSN 0741-3106.

[22] GU, X. et al. On-chip compensation of self-heating effects in microbolometer infrared detector arrays. *Sensors and Actuators A: Physical*, 1998, vol. 69, no. 1, pp. 92-96. ISSN 0924-4247.

[23] HWANG, S. J. et al. High performance read-out IC design for IR image sensor applications. *Analog Integr. Circuits Signal Process.*, 2010, vol. 64, no. 2, pp. 147-152. ISSN 0925-1030.

[24] AMAND E. L., T. C. J. *The Theory behind FTIR Analysis* [online]. Goteborg, 2007 [cit. 857-50115.

[25] SETTLE F.A. *Handbook of Instrumental Techniques for Analytical Chemistry*. 2. Arlignton: Prentice Hall, 1997. 1024 pp. ISBN 0-13-1777338-0.

[26] STUART B. *Infrared Spectroscopy: Fundamentals and Applocations*. 3. John Wiley & Sons, Ltd, 2004. 223 pp. ISBN 0-470-85427-8.

[27] CLEIN, D. *CMOS IC Layout*. Newnes, 2000. pp. ISBN 0-7506-7194-7.

[28] PAUW, L. J. V. D. Method of Measuring Specific Resistivity and Hall Effect of Discs of Arbitraty Shape. *Philips Research Reports*, 1958, vol. 13, no. 1, pp. 9.

[29] LIVERMORE C., V. J. Material Properties Database. [online]. 5.11.2013 [cit. Available from: <http://www.mit.edu/~6.777/matprops/matprops.htm>.